



**HAL**  
open science

# Synthesis and physicochemical characterization of new calcined layered double hydroxide Mg Zn Co Al-CO<sub>3</sub>; classical modeling and statistical physics of nitrate adsorption

Mounira Elhachemi, Zoubida Chemat-Djenni, Derradji Chebli, Abdallah Bouguettoucha, Abdeltif Amrane

## ► To cite this version:

Mounira Elhachemi, Zoubida Chemat-Djenni, Derradji Chebli, Abdallah Bouguettoucha, Abdeltif Amrane. Synthesis and physicochemical characterization of new calcined layered double hydroxide Mg Zn Co Al-CO<sub>3</sub>; classical modeling and statistical physics of nitrate adsorption. *Inorganic Chemistry Communications*, 2022, 145, pp.109549. 10.1016/j.inoche.2022.109549 . hal-03985515

**HAL Id: hal-03985515**

**<https://hal.science/hal-03985515>**

Submitted on 17 Feb 2023

**HAL** is a multi-disciplinary open access archive for the deposit and dissemination of scientific research documents, whether they are published or not. The documents may come from teaching and research institutions in France or abroad, or from public or private research centers.

L'archive ouverte pluridisciplinaire **HAL**, est destinée au dépôt et à la diffusion de documents scientifiques de niveau recherche, publiés ou non, émanant des établissements d'enseignement et de recherche français ou étrangers, des laboratoires publics ou privés.



Distributed under a Creative Commons Attribution - NonCommercial 4.0 International License

## Synthesis and physicochemical characterization of new calcined layered double hydroxide MgZnCoAl-CO<sub>3</sub>; Classical modeling and statistical physics of nitrate adsorption

Mounira Elhachmi<sup>1</sup>, Zoubida Chemat<sup>1</sup>, Derradji Chebli<sup>2</sup>, Abdallah Bouguettoucha<sup>2</sup>, Amrane Abdeltif<sup>3</sup>

<sup>1</sup>Laboratoire d'analyse fonctionnelle des procédés chimiques. Département de génie des procédés. Faculté de technologie. Université Saad Dahleb Blida, B .P 270 route de Soumaa, Blida, Algérie

E-mails : monicaelhachmi@gmail.com

<sup>2</sup>Laboratoire de Génie des Procédés Chimiques (LGPC) Faculté de Technologie, Département de Génie des Procédés, Université Ferhat Abbas, Sétif, Algérie

E-mails :; *abdallah.bouguettoucha@univ-setif.dz; derradji\_chebli@yahoo.fr; m.guediri@univ-setif.dz;*

<sup>3</sup>Univ Rennes, Ecole Nationale Supérieure de Chimie de Rennes, CNRS, ISCR (Institut des Sciences Chimiques de Rennes)-UMR 6226, F-35000 Rennes, France

*E-mail: abdeltif.amrane@univ-rennes1.fr*

### Abstract

This research focuses on the study of a new material, a layered double hydroxide, which was synthesized using a co-precipitation method at pH constant and, then, tested for its retention of nitrate anions. The LDH was prepared from four metal cations Mg-Zn-Co-Al to produce the quadratic material mentioned, MgZnCoAl-CO<sub>3</sub>, which was calcinated to obtain metal oxides. Different techniques of characterization were used such as FTIR, X-ray diffraction, BET, SEM and EDX. Adsorption experiments for nitrate were carried out to test the effect of contact time, adsorbent mass, initial pH value of the solution and the temperature on the adsorbent process in synthetic solutions with various levels of nitrate ranging from 100 to 200mg/L to find the optimal conditions. The results of our research shows that 72.73% of nitrate can be removed under neutral conditions, in a 100mg LDH and 100ml nitrate solution with initial concentration of 100mg/l at a temperature of 25°C. Our kinetic data best fitted the Pseudo-Second Order model. The intraparticle diffusion model shows that adsorption kinetics was dictated by external and intraparticle diffusion. The Sips model was the adsorption isotherm which best fitted the results of our experiments. Furthermore, it was observed that the adsorption of nitrates decreased in the presence of competitive anions in the order of phosphate > sulphate. Finally, for a deeper insight in the nitrate adsorption mechanism, the statistical physics model was used to

quantify the number of adsorbed nitrate molecules per site, the anchorage number, the receptor sites density, the adsorbed quantity at saturation, the concentration at half saturation and the molar adsorption energy. A detailed thermodynamic analysis was performed demonstrating that the adsorption mechanism was endothermic and associated to physical forces. The thermodynamic analysis confirmed the feasibility and spontaneous nature of the adsorption of nitrate on tested adsorbent.

Keywords: Layered double hydroxides; Adsorption; Statistical physics models; Nitrate;

## 1. Introduction

Layered double hydroxides have been the subject of intense study for several years due to their electrochemical and anion exchange properties(1)(2). LDHs consist of a family of compounds formed by a layering of Brucite-like  $Mg(OH)_2$  sheets in which a fraction of the divalent metal is substituted by a trivalent metal, thus creating a surplus of positive charges which are stabilized by the presence of hydrated anions found in the interlayers(3)(4). LDHs can be represented by the general formula:  $[M^{2+}_{1-x} M^{3+}_x (OH)_2]^{x+} [A^{n-}_{x/n} \cdot m H_2O]^{x-}$ ;  $x=n$  ( $M^{3+}$ )/ $n$  ( $M^{2+} + M^{3+}$ ). Where  $M^{2+}$  is a divalent metal such as  $Mg^{2+}$ ,  $Fe^{2+}$ ,  $Co^{2+}$ ,  $Ni^{2+}$ ;  $M^{3+}$  is a trivalent metal  $Al^{3+}$ ,  $Cr^{3+}$ ,  $Fe^{3+}$ ;  $A^{n-}$  represents the compensatory anion  $CO_3^{2-}$ ,  $Cl^-$ ,  $NO_3^-$ ;  $n$  is the layer charge while  $m$  represents the number of water molecules. In the majority of cases,  $x$  usually has a value of between 0.10 and 0.33(5)(6). The flexible nature of the interlayer space gives the material a high anion exchange capacity (7). This is determined by the interlayered anion initially present in the sample, the density of the layer charge and the cationic nature of the layer. Three different anion capture mechanisms can be identified: anionic exchange, adsorption and the reconstruction of calcinated LDH by memory effect. Thus, numerous molecules can be captured such as anions of both an organic and inorganic nature.

The areas of application for LDH materials are extremely varied. They were first used as catalysts in the chemical industry and as anion exchangers in pharmaceutical applications. They have also proved to be very efficient in capturing pollutants, such as nitrate (8)(9)(10); phosphate (11)(12)(13); chromate (14)(15) as well as other organic pollutants such as pesticides and herbicides (16) when used in environmental remediation processes.

Nitrates are extremely dangerous to the environment, especially when their concentration is very high. Due to its water solubility, the nitrate ion is the most commonly found pollutant of underground water in the world, constituting a serious threat to drinking water and causing ecological disruption(17). High concentrations of  $NO_3^-$  in drinking water can threaten public health and the environment. High levels of  $NO_3^-$  have been known to stimulate the growth of algae which causes eutrophication of the waterways(18). Intense fertilization of the soil on some agricultural plains together with the dumping of both industrial and domestic effluent has increased the level of nitrate in both surface and subterranean water in several regions of the world. Consequently, the European Union has set a limit for nitrate in drinking water at 50mg/L(19).

There exist several conventional procedures to eliminate nitrates from contaminated water, such as biological denitrification, as well as several physio-chemical methods based on membrane processes like inverse osmosis and electrodialysis. However, ion exchange and electrolysis have several drawbacks: incomplete elimination, the need for high levels of energy and high, or costly doses of reactive(20). Adsorption is, therefore, the method which has proved itself to be the most effective in eliminating nitrates, especially when a cheap adsorbent is used.

To understand the adsorption process in the first time, classical interpretations were developed using empirical models describing the nitrate adsorption process (21). The monolayer models developed from statistical physics theory have been implemented to analyze the adsorption isotherms of this anion at different temperatures. These models were used to assign interpretations at the microscopic scale of the nitrate ion adsorption mechanism via steric and energetic physicochemical parameters (22)(23).

In this study, four cationic precursors were used in the preparation of the LDH. The isomorphous substitution of one metal with another improves the redox and acid-base properties of the LDH which are essential for both catalysis and adsorption. The MgZnCoAl-CO<sub>3</sub> LDHs were calcinated at 500°C and added to nitrate solutions. The performance of the LDH to remove nitrate from the solution was examined in relation to several factors (temperature, dose, time, pH value, presence of other anions).

## **2. Materials and Methods**

### **2.1. Preparation of the ZnMgCoAl-CO<sub>3</sub> adsorbent:**

The preparation of the MgZnCoAl-CO<sub>3</sub>, with a molar ratio of 2 (Mg<sup>2+</sup> + Zn<sup>2+</sup> + Co<sup>2+</sup>)/(Al<sup>2+</sup>) was carried out by using the co-precipitation method (24). Described thus: MgCl<sub>2</sub>.6H<sub>2</sub>O (0.22M), ZnCl<sub>2</sub>.6H<sub>2</sub>O (0.22M), CoCl<sub>2</sub>.6H<sub>2</sub>O (0.22M) and AlCl<sub>3</sub>.6H<sub>2</sub>O (0.33M) were dissolved in 500ml of distilled water. The pH of the reaction mixture was kept constant at 10.0 by simultaneously adding 500mL of NaOH(2M) and Na<sub>2</sub>CO<sub>3</sub>(1M) solution. After a maturing time of 24 hours, the clay was centrifuged and, then, washed with deionized water until obtaining MgZnCoAl-CO<sub>3</sub> without Cl<sup>-</sup> (confirmed by a AgNO<sub>3</sub> test). It was finally dried at a temperature of 85°C for 18 hours, then crushed and passed through a 100 mesh sieve to produce the MgZnCoAl-CO<sub>3</sub> product. The LDH obtained was calcinated at 550°C for 4 hours in order to improve both its texture and structural properties. It was then decarbonated and dehydrated to obtain a MgZnCoAl-C with increased anion exchange capacity. The final product was called CLDH.

### **2.2. Characterization of MgZnCoAl-CO<sub>3</sub>hydrotalcite**

The point of zero charge (pHpzc) was determined by using a method described by Chebli et al(25).50ml of distilled water was added to 50mg of the adsorbent and poured into several Erlenmeyer flasks. Then, either 0.1M HCl or 0.1M NaOH was added to each flask to adjust the pH value of the solution between 2 and 12. After 24 hours of mixing, the final pH value was measured.

Morphological analysis using X-ray diffraction (XRD) is carried out using Bruker D8 diffractometer with Cu K $\alpha$  radiation ( $\lambda= 0.15418$  nm) and at scan speed of 5°/min from  $2\theta= 2^\circ$  to  $2\theta=70^\circ$  (40 kV and 30 mA).FTIR adsorption spectra were recorded between 4,000 and 400cm<sup>-1</sup> by means of a Perkin Elmer FTIR spectrophotometer (SPECTRUM RX-1). Surface area, pore volume and pore size analysis were performed by an ASAP 2020 Brunauer–Emmett–Teller (BET). The BET technique was adopted to measure the specific surface area (SSA) and the BJH method, using the N<sub>2</sub> adsorption and desorption isotherms, was used to measure the pore sizes and the volumes of LDH and CLDH.Scanning electron micrographs SEM of the sample was obtained by FEI QUANTA 650 scanning electron microscope operating at 30 kV.

### **2.3. Nitrate solutions:**

The experiments were carried out using commercially available potassium nitrate (PanReac). To prepare 1000mg/L of stock nitrate solution, NO<sub>3</sub>, 1.6305g of KNO<sub>3</sub> was dissolved in 1litre of distilled water. The stock solution underwent a serial dilution to obtain the required concentration of nitrate.

### **2.4. The effect of pH on the adsorption process:**

The pH of the contact solution is an important parameter in the adsorption process. The effect of pH on the adsorption of nitrate on MgZnCoAl-C was studied in an initial range of solutions whose pH varied between4 to 12. A mass of 100mg of material was added to 100ml of solution with an initial nitrateconcentration of 100mg/L. The experiments were carried out by stirring all the mixtures at  $25 \pm 1^\circ\text{C}$ . The initial pH value was adjusted by the serial addition of NaOH or HCl solution. The concentration of the residual nitrate ions was determined spectrophotometrically, according to Rodier protocol, using a DR/2000 model (Hach Spectrophotometer Selecta)(26).

### **2.5 The effect of the adsorbent dosage on the adsorption process:**

The effect of the adsorption dosage, on the adsorption of the nitrate onto MgZnCoAl-CLDH was studied in different solutions having a pH value 6 and stirred at  $25 \pm 1^\circ\text{C}$  for 5 hours. The nitrate concentration of the solutions was 100mg/L while the concentration of MgZnCoAl-CLDH was between 50 and 300mg/L.

## 2.6 Kinetics of Nitrate Adsorption:

The adsorption equilibrium of the MgZnCoAl-C adsorbent was measured through a series of batch adsorption experiments. The adsorption kinetics was measured by adding 100mg of the sample material to 100ml of nitrate solution (100mg/L) which was vigorously stirred at a speed of 200rpm throughout the whole of the reaction time. At the end of the mixing time, the sample was centrifuged. All the experiments were duplicated twice to ensure reproducibility of the data. The adsorption capacity at time  $t$ ,  $Q_t(\text{mg/g})$  and the percentage of nitrate removed by the adsorbent were calculated by applying equations (1) and (2) respectively:

$$Q_t = (C_0 - C_t) \frac{V}{m} \quad (1)$$

$$\% \text{Removal} = 100 \frac{C_0 - C_t}{C_0} \quad (2)$$

Where  $C_0$  is initial nitrate concentration (mg/L),  $C_t$  (mg/L) is the residual concentration at time  $t$ ,  $V$  (mL) the volume of solution and  $m$  is the mass (mg) of adsorbent.

The adsorption kinetics of nitrates on LDH was studied through the application of several kinetic models, such as the pseudo-First Order (PFO) (27), the Pseudo-Second Order (PSO) (28), Elovich(29) and the intraparticle diffusion model (IPD)(30), in order to determine the rate constant of nitrates and investigate the mechanisms of the reaction(31)(32). These models 3; 4; 5; 6 are represented in table 1.

where  $Q_e$  and  $Q_t$  are the amount of nitrates adsorbed onto adsorbent at the equilibrium time and at time  $t$  (min), respectively,  $k_1$  is the rate constant of the PFO model,  $k_2$  is the rate constant of the PSO model, and  $k_3$  is the IPD rate constant,  $\alpha$  is the initial adsorption rate (mg/g min) and  $\beta$  is the desorption constant are the Elovich coefficients.  $C$  is the intercept.  $\beta_t$  is a mathematical function.

The adsorption speed ( $h_0$ ) for the PFO (mg/g min) and PSO (mg/g min) model can be calculated from the following equations:

$$H_0 = K_1 \times Q_e \quad (7)$$

$$H_0 = K_2 \times Q_e^2 \quad (8)$$

## 2.7 Adsorption Isotherms:

Equilibrium studies or adsorption isotherms, as known, is an important aspect for adsorption studies, it helps to describe the adsorbent-adsorbate interaction and provides information on the maximum capacity of adsorption. A constant amount of MgZnCoAl-C (100mg), with different initial concentrations (varying between 10-300 mg/L), was mixed with a constant volume of nitrate solution (100 mL). These suspensions, all with a pH value of 6, were shaken at a temperature of  $25 \pm 1^\circ\text{C}$  for 5 hours, and then centrifuged. The amount of nitrates adsorbed at equilibrium,  $Q_e$  was calculated by using the following equation 9:

$$Q_e = (C_0 - C_e) \frac{V}{m} \quad (9)$$

Where  $C_e$  is the final nitrate concentration (mg/L).

## 2.8. Isotherms analysis

Mathematical simulations were considered to evaluate accurately the interaction between the LDHs and the Nitrate ions.

### 2.8.1. Classical nitrate adsorption isotherm model:

Adsorption isotherm data were fitted by nonlinear regression analysis using four models: Langmuir (33), Freundlich(34), Sips (35), and Redlich-Peterson (36). These models are presented in table 2:

Where  $Q_m$  is the maximum adsorption capacity (mg/g),  $K_L$  is the Langmuir constant,  $K_F$  (in  $(\text{mg/g})(\text{L/mg})^{1/n}$ ) and  $n$  are Freundlich constants,  $R$  is the universal gas constant (J/mol.K),  $T$  is the temperature (K),  $A_{GP}$  (L/mol),  $B_{RP}$  (L/mol), and  $g$  are constants of Redlich-Peterson model,  $K_S$   $((\text{L/g})^{\beta S})$  and  $m_s$  are Sips constants.

An essential characteristic parameter, called the separation factor  $R_L$ , can be calculated for the Langmuir model. It predicts the feasibility of adsorption process: for  $0 < R_L < 1$ , the process is favorable, irreversible if  $R_L = 0$ , linear if  $R_L = 1$  or unfavorable if  $R_L > 1$ . The  $R_L$  expression is given by the equation:

$$R_L = \frac{1}{1 + K_L C_0} \quad (14)$$

## 2.8.2. Statistical physics analysis

Adsorption models are important in the design and classification of the adsorption processes. However, the mechanisms of the adsorption process can only be partially understood by using traditional adsorption models (eg. Langmuir, Freundlich or Sips). Therefore, three theoretical models have been successfully applied to obtain a possible correlation between the characterization of the adsorbents, their adsorption properties and the adsorption mechanisms. Any contact between a solute and an adsorbent is always followed by a reaction where a variable number of molecules will be adsorbed on  $N_M$  receptors per unit mass of adsorbent. thus equation (15) schematizes this reaction where (A) represents the solute adsorbed on the receptor site (S) and (n) the number of molecules or quite simply the stoichiometric coefficient which can take any higher or lower value a 1 depending on the type of anchoring of the molecule on the surface of the adsorbent material either multimolecule by site or fraction of molecule by site(37).



In this study, the basis of calculation is based on the use of the grand canonical partition function describing the microscopic adsorption process. The receptor site is assumed to be empty or occupied by one or more molecules. Thus, we define the state of occupation number  $N_i$  which expresses the situation in which its receptor site is found (38). In this case three models of physical statistics are used.

### **Model 1: Monolayer adsorption model with one binding site for nitrate removal:**

This model assumed that the nitrate adsorption occurred by a formation of one adsorbed layer with a single energy (39). It was also supposed that each contributing receptor site in the adsorption can capture a variable number of nitrate anions defined by the parameter n. The variation of the adsorbed quantity as function of the equilibrium concentration is given by the expression in table 3

The adsorbed anion quantity at saturation ( $N_{sat}$ ) can be calculated by:

$$Q_{sat} = nN_M \quad (16)$$

**Model 2: Monolayer adsorption model with two binding sites for nitrate removal:**

It was supposed that two different functional groups participated in the adsorption of  $\text{NO}_3$  anions on tested LDH. In this case, two adsorption energies were involved for each type of functionalities. Two types of functional group densities were considered ( $N_{m1}$  and  $N_{m2}$ ) where it was also assumed that the first and second adsorption sites can select  $n_1$  and  $n_2$  adsorbates during the nitrate anions removal, respectively. According to these hypotheses, the mathematical expression of this second model, is summarized in table 3.

**Model 3: Monolayer adsorption model with three binding sites for nitrate removal:**

It was proposed that a third functional group can contribute to the adsorption of nitrate anions. The expression for this model is given in table 3:

where  $n_1$ ,  $n_2$  and  $n_3$  are the numbers of ions adsorbed by each type of binding site from LDH surface, respectively.

Where  $n$  is the number of adsorbed molecules per site,  $C_{1/2}$  (mg/L) is the concentration at half saturation,  $N_m$  (mg/g) is the receptor site density,  $Q_e$  is the adsorbed amount and  $C_e$  (mg/L) is the concentration at equilibrium

The parameters  $n_1$ ,  $n_2$  and  $n_3$  describe the number of adsorbed nitrate ions per the first and second functional groups of LDH,  $N_{m1}$ ,  $N_{m2}$  and  $N_{m3}$  are the densities of saturated functional groups and two concentrations at half-saturation are reported in the model, which are defined as  $C_1$ ,  $C_2$  and  $C_3$ .

**2.9 Thermodynamics****3.9.1. Adsorption Thermodynamics:**

Temperature is one of the most important parameters of the adsorption process. Thermodynamic parameters, such as Gibbs free energy change ( $\Delta G^\circ$ ), standard enthalpy ( $\Delta H^\circ$ ) and standard entropy ( $\Delta S^\circ$ ) were studied to better understand the effect of temperature on the adsorption process. Experiments were carried out on samples containing 100mg/L nitrate and 100mg of the adsorbent, MgZnCoAl-C at different temperatures: 15°C, 25°C, 40 and 50°C  $\pm$  1°C. The thermodynamic parameters  $\Delta G^\circ$ ,  $\Delta H^\circ$  and  $\Delta S^\circ$  were calculated using equation in table 4 (43).

Where  $R$  is the universal gas constant (8.314 J.mol<sup>-1</sup>.K<sup>-1</sup>),  $T$  is the temperature (°K),  $K_D$  is the thermodynamic equilibrium constant. The values of  $K_D$  were estimated from the best fit

parameters of isothermal model.  $S_a$ , Entropy.  $K_B$ , Boltzmann constant (J/K).  $G$ , Gibbs free enthalpy,  $Z_v$ , Translation partition function per volume unit.  $Z_{gr}$ : The translation partition function.  $V$ : Volume(L).  $h$ : Planck constant (J/s),  $m$ : Adsorbent mass (g). **E<sub>int</sub>**: internal energy (J/mol)

### 2.10 Selectivity of the LDH for nitrate:

The results of the adsorption process discussed below concern only the nitrate ion. However, in reality, water contains several other anions which all compete in the adsorption process. In order to observe the effect these interfering ions have on the adsorption of the nitrate, a combination of known quantities of some of the ions most commonly found in water, such as phosphate and sulfate, were added, along with 100mg of MgZnCoAl-C, to the nitrate solution. The initial concentration of nitrate was fixed at 100mg/L while the initial concentration of the other anions varied between 50mg/l and 200mg/L.

## 3. Résultats et discussion :

### 3.1 Caractérisation of MgZnCoAl-CO<sub>3</sub> :

The point of zero charge (pH<sub>pzc</sub>) of the adsorbent was reported on a (pH<sub>e</sub> – pH<sub>i</sub>) = f(pH<sub>i</sub>) plot (Fig. 1). The values of pH<sub>pzc</sub> for MgZnCoAl-CO<sub>3</sub> and MgZnCoAl-C phases are 8.04 and 8.82, respectively. Below the pH<sub>pzc</sub>, the surface of MgZnCoAl-C was positively charged and thus effective in removing negatively charged species from aqueous solution. While at pH values above the pH<sub>pzc</sub>, the MgZnCoAl-C surface was negatively charged.

The X-ray powder diffraction pattern for the LDH and the CLDH (obtained after calcination at 500°C) and for the LDH after the adsorption of the nitrate ions are illustrated in Fig. 2. The XRD patterns for the non-calcinated phase MgZnCoAl-CO<sub>3</sub> show sharp and symmetrical peaks on the same basal planes (003), (006) and (012) corresponding to  $2\theta = 11.62^\circ$ ,  $23.26^\circ$  and  $36.58^\circ$ , respectively, which indicates the reticular distances  $d_{hkl}$  [ $d(003) = 2d(006)$ ] and allows access to the parameters of the hexagonal lattice  $c = 3d(003) = 22.8\text{Å}$ . These peaks, which are characteristic of the hydrotalcite phase, confirm the well-crystalline, layered structure of the product; a result that has been recorded by several other authors in their research (13)(44). Asymmetrical peaks on non-basal planes (015), (018), (110) and (113) were recorded at higher angles ( $38.96^\circ$ ,  $48.44^\circ$ ,  $60.56^\circ$  and  $61.83^\circ$ ).

In the spectrum for the calcinated phase, MgZnCoAl-C, the peaks (003), (006) and (012)(45) are absent which indicates that calcination has profoundly modified the crystalline

structure of the LDHs. In fact, high temperatures cause dehydration, dihydroxylation and the release of interlayer anions which all contribute to the decomposition of the layered structure(46).

Three major peaks, occurring on the reflection planes (111), (200) and (220)(47) at around  $2\theta = 35^\circ$ ,  $43^\circ$  and  $63^\circ$ , respectively, can be attributed to the original mixture of metal oxides, (MgO), (ZnO) and (CO<sub>3</sub>O<sub>4</sub>)(48), in the amorphous phase. However, after nitrate adsorption, the characteristic peaks of the LDHs re-appear confirming the reconstruction of the MgZnCoAl-C structure due to the “memory effect”(49).

The FT-IR spectra of the prepared samples are illustrated in Fig.3. The broad band, which appeared on the LDH spectrum at around  $3,488\text{cm}^{-1}$ , was attributed to the asymmetric and symmetric stretching mode of the O-H bond in the hydroxyl groups which make up the LDH layers and the interlayer water molecules (50)(51). The bending vibration of the interlayer H<sub>2</sub>O was reflected in the broad bands that appeared at  $1,630\text{cm}^{-1}$ . The sharp and symmetric peak at  $1353\text{cm}^{-1}$  reflected the vibrations of the CO<sub>3</sub><sup>2-</sup> interlayer anions (52). A band, corresponding to the stretching mode of the metal-oxygen bond appeared below  $700\text{cm}^{-1}$ . The sharp bands appearing between  $500\text{cm}^{-1}$  and  $700\text{cm}^{-1}$  were caused by the lattice vibrations characteristic of the hydroxide sheets.

A profile analysis for the IR spectrum of the calcined LDH sample revealed a significant decrease in the intensity of the bands at  $\sim 3,488$  and  $\sim 1,630\text{cm}^{-1}$  indicating both dihydroxylation and dehydration of the product. Furthermore, the characteristic adsorption peaks, observed at  $\sim 3,000\text{cm}^{-1}$  and  $\sim 1,000\text{cm}^{-1}$ , disappeared, suggesting surface decarboxylation. In accordance with the XRD analysis, these results confirm that the structure of the LDH was completely destroyed during the calcination process. A band, associated with the antisymmetric stretching mode of nitrate ( $\nu_3$ ), appeared at 1384, confirming the adsorption of the nitrate ions onto the MgZnCoAl-C (53).

The results of N<sub>2</sub> adsorption-desorption isotherms of the LDH and the CLDH at 77K while SSA are represented in Fig.4, pore volumes and pore sizes are included in Table 5. Following the classification system of Sing et al(54), the isotherms for the prepared materials were classified as Type IV, presenting H<sub>3</sub> type hysteresis loops at high relative pressure P/P°. This indicates the presence of a mesoporous structure with non-rigid aggregates of plate-like particles with slit-shaped pores of varying shape and size(55)(56). Table 5 shows that the Brunauer-Emmett-Teller (BET) surfaces of the calcined samples are larger than those of the

non-calcined samples due to the effect of thermal treatment on the sample at 773°K. The dehydration and decarbonation that occur during calcination, can cause the formation of channels and pores, which increase the specific surface area of the calcined sample. These results correspond to the findings recorded in related literature(57)(58).

A scanning electron microscope was used to analyse the two LDHs (MgZnCoAl-CO<sub>3</sub> and MgZnCoAl-C),Fig.5. A study of the various signals confirmed the shape of the particles, lamination and the surface topography of the samples. The images taken of the particles show that the primary particles consist of hexagonal discs, synthesized by the co-precipitation method.Calcination has made them lose both their form and their crystallinity and their extremely perforated surface is due to an increase in the internal, and external, specific surface area.

During the calcination process, water molecules remaining within the structure of the LDH will evaporate, allowing it to become more compact, resulting in a decrease in the size of the particles. The structure becomes amorphous (breakdown of the LDH structure) which is consistent with the results of the diffractogram. The process makes the material more porous in nature(59).

The spectrum illustrated in Fig.5. corresponds to the EDX analysis of the elemental composition of the MgZnCoAl-C sample. It confirms the presence of different amounts of the four metal cations (magnesium, aluminium, zinc, cobalt). The presence of the O ion indicates oxidation of the mixed metals after calcination.

### **3.2 Effect of pH:**

The pH value is one of the most important parameters in the physiochemical reaction at the water-solid interface. Our research was carried out using solutions of pH value  $\geq 5$  because LDHs are generally unstable in the acidic medium Fig .6. shows the findings of our research. According to these results, the nitrate removal efficiency of the LDH changes when pH values increase from 5 to 12. It can be seen that the amount of nitrate adsorbed by MgZnCoAl-C decreased from 35mg/g to 18,23mg/g when the pH value increased from 6 to 12. This indicates that the adsorption process was favorable in a neutral medium(60) , indicating a strong interaction between the negatively charged nitrate ions and the positively charged adsorbent surface ( $\text{pH}_{\text{sol}} < \text{pH}_{\text{pzc}}$ ). In our study, the  $\text{pH}_{\text{pzc}}$  was found to be 8.82. When the pH value is below that of the  $\text{pH}_{\text{pzc}}$ , the superficial area of the adsorbent is protonated. Hence, it acquires a positive charge, enhancing the adsorption of the negatively charged nitrate ions by electrostatic attraction. However, when the pH value is greater than the  $\text{pH}_{\text{pzc}}$ , the superficial area of the

adsorbent is deprotonated. As a result, it acquires a negative charge, becoming unfavorable to the adsorption of nitrate ions which are themselves negatively charged. The above data suggests that 6 is the optimal pH value for the removal of nitrates from aqueous solutions(61)(62).

### 3.3 Effect of adsorbent dosage:

Adsorbent dosage is an important consideration since it is directly linked to the cost factor of large projects and impacts the quantity of nitrates adsorbed and their percentage removal, as is represented in fig .7. It can be seen that the nitrate removal efficiency of the LDH increases as its dosage increases from 20 to 300mg. Although this corresponds to an increase in active sites for adsorption, but the value of the amount of adsorption has decreased. Our research shows that the best result for nitrate removal was in a solution where the concentration was 300mg LDH which managed to eliminate 80.45% of the ions. When the dosage of the adsorbent is high, a very rapid but superficial adsorption occurs on the surface of the adsorbent resulting in a low adsorption capacity. Thus, with weak doses of the adsorbent, the quantity of the nitrate adsorbed per unit mass of the  $\text{MgZnCoAl-CO}_3$  increased, causing an increase in the  $Q_e$  value(63)(64).

### 3.4. Effects of contact time:

The adsorption of nitrate onto MgZnCoAl-C was studied at different contact times in three different nitrate solutions with initial concentrations of 50mg/L, 100mg/L and 200mg/L, keeping all other parameters constant. The results are shown in Fig.8. It can be seen that the adsorption process took place in two stages: the first, rapid; the second, slow. The quantities of nitrate adsorbed increased in relation to an increase in contact time. The curve shows that the rate of nitrate removal increased rapidly in the first 60 minutes and reached equilibrium after 300 min (5h) with high fixation. The quantities adsorbed were recorded as 30.9mg/g, 36mg/g and 46.9mg/g for initial nitrate concentrations of 50mg/L, 100mg/L and 200mg/L, respectively.

### 3.5. Adsorption kinetics

Fig.9, shows compatibility to the PFO, PSO and Elovich models. Table 6 summarizes the kinetic parameters derived from these models.

A study of the  $R^2$  values in Table 6 shows that both the Pseudo-first Order and Elovich model have weak correlation coefficients compared to the Pseudo-second Order model, which presents a very strong correlation coefficient of over 0.99; this confirms that the pseudo-second order model fits well with our experimental data (fig.6). Moreover, for all the concentrations under study, the calculated adsorption capacity given by the pseudo-second order model ( $Q_e$ ) was extremely close to the empirical adsorption capacity,  $Q_{exp}$ . Consequently, with a  $R^2$  value

close to 1, the pseudo-second order model was best fitted to describe the adsorption kinetics of nitrate onto the CLDH, and suggested a physisorption mechanism.

The intraparticle diffusion model was used to highlight the mechanism of nitrate adsorption onto MgZnCoAl-C. Fig.10. plots the adsorbed amount ( $Q_t$ ) as a function of ( $t^{0.5}$ ) for all three samples and shows that the two linear plots do not cross the origin. According to the results, intraparticle diffusion may consists of two steps: step one takes place in the period  $t^{1/2} < 6$  and involves the external diffusion of nitrate molecules to the surface; step two, in the range of  $6 < t^{1/2} < 11$ , consists of the slow adsorption of molecules until equilibrium is reached(65). The correlation coefficients  $R^2$  and the rate constants ( $K_3$ ) for the intraparticle diffusion were determined by studying the slope of the respective plots. They are summarized in table 6. The  $K_3$  values recorded in Table 1 are between 0.277 and 0.757 mg/g min<sup>1/2</sup>. It is clear that, as the concentration of the nitrate ions increases, the  $K_3$  value becomes larger due to a process of diffusion (66). The values of intercept C (Table 6) provide information about both the boundary layer thickness (ie. the larger the intercept, the greater the effect of the boundary layer) and the external mass transfer resistance. The results show that the constant C increases from 24.8 to 30.08 as the concentration of the nitrate increases from 50 to 200mg/L.

### 3.6 Classical adsorption isotherms models:

The adsorption isotherm was used to determine the distribution of nitrate between solution and solid phases of the LDHs. Adsorption isotherm data were fitted by nonlinear regression analysis using four models: Langmuir, Freundlich, Sips, and Redlich-Peterson. These models are presented by the following figures.

Fig. 11, shows the adsorption isotherms for nitrate onto MgZnCoAl-C, studied at three different temperatures, 15°C, 25°C and 40°C, but keeping all the other parameters constant. All the isotherms were deemed favorable since the  $Q_e$  values increased with  $C_e$ . The isotherms exhibited a plateau at high  $C_e$  values, indicating that all the active sites for adsorption were completely occupied. According to the classification of the liquid-solid isotherms established by (Giles et al) (67). The isotherms that represent the adsorption of nitrate ions onto MgZnCoAl-C may be classified as L-type, or Langmuir, which are the isotherms most commonly used for solute adsorption. Table 7 gives the values of  $Q_m$ , the correlation coefficient  $R^2$ , AIC and all other parameters of the isotherms used in our study.

The value of  $Q_m$  derived from the Langmuir model is 51.10 mg/g at 25°C which provided the best fit for our experimental data. The  $R_L$  value ( $0.1 < R_L < 0.75$ ) indicates a favorable adsorption of nitrates onto the MgZnCoAl-CO<sub>3</sub> LDH. The parameters n of the Freundlich model, known as the heterogeneity factor, were used to define the mechanism of the

adsorption process i.e. linear ( $n=1$ ); chemical ( $n<1$ ); physical ( $n>1$ ). The Redlich-Peterson isotherm, which incorporates elements from the Langmuir and Freundlich models, was used in our study to cancel out any inaccuracies and improve the fit between the two equations.

Of the four models, the Sips model was selected to represent the adsorption isotherms gave the best correlation with  $R^2$  value of 0.998 and AIC value of 17.45 at a temperature of 40 °C. This model combines both the Langmuir and Freundlich isotherms to predict the adsorption capacity in a monolayer where the adsorbate concentration is high. It is a three-parameter isotherm and is used to describe the adsorption process on heterogeneous surfaces (68). The maximum adsorbent capacity predicted by the Sips model was 55.97mg/g<sup>-1</sup> at 40°C.

Table 8, compares the maximum adsorption capacity of calcined MgZnCoAl-LDH samples for nitrate in our study to the nitrate removal capacity of other calcined and uncalcined LDH samples recorded in the literature. This comparison confirms that calcined MgZnCoAl LDH is a highly promising material and is extremely competitive owing to its simple, low-cost synthesis, its thermal stability and its reconstruction properties.

### 3.7 Statistical physics analysis:

Three models were applied to fit the experimental adsorption data of nitrate anions for three temperatures, 15°C, 25°C and 40°C, and is shown in fig.12 where the determination coefficients  $R^2$  ranged from 0.989 to 0.997 for these correlations. However, model 1 and model 3 did not show a clear evolution of their parameters thus being improper to understand the adsorption mechanism. On the other hand, the monolayer adsorption models with two binding sites showed the best performance and the trends of its physicochemical parameters with respect to temperature were interpreted to characterize and explain the corresponding adsorption mechanism of nitrate ions. All Parameters of three models are summarized in the following Tables 9, 10, 11 respectively.

The parameter  $n$  is a stoichiometric coefficient that represents the number of nitrate anions bound to the adsorption sites of the LDH. It can be used to describe the interaction way of nitrate anion with both adsorption sites. According to the literature(71), three scenarios can be analyzed:

a) if  $n_1 < 0.5$ , This case reflected a parallel adsorption orientation on LDH adsorbent surfaces (i.e., the adsorbate can interact with at least two adsorption sites).

- b) If  $0.5 < n_i < 1$ , the nitrate anions can be adsorbed via mixed orientation (parallel and non-parallel orientations) with two different percentages.
- c) If  $n_i > 1$ , This situation implies that nitrate anions can be adsorbed with a non-parallel orientation (i.e. the adsorbate can interact with one adsorption site).

In the case where the number  $n$  is less than 0.5, we speak of parallel adsorption on the HDL surfaces (i.e. the adsorbate can interact with at least two adsorption sites ), while if the number  $n$  is between 0.5 and 1, the nitrate ions will be adsorbed by mixed orientations (parallel and non-parallel orientations) with two different percentages, however for numbers  $n$  greater than 1 the nitrate ions can be adsorbed with a non-parallel orientation (i.e. the adsorbate can interact with an adsorption site).

### 3.8 Energetic (E) parameter:

The interactions between the nitrate molecules and the MgZnCoAl-C surface could be explained through the adsorption energy (72)(73) estimation from the equation:

$$\Delta E = RT \ln\left(\frac{C_s}{C_0}\right) \quad (25)$$

Where  $C_s$  is the solubility of the studied adsorbate and  $C_{1/2}$  is the half-saturation concentration obtained by the adjustment method and  $R = 8.314 \text{ J/mol K}$  is the ideal gas constant respectively. Calculated adsorption energies reported in Table 10 and Fig. 11(d) illustrate the evolution of these energies as a function of temperature.

All  $\Delta E_1$  and  $\Delta E_2$  values were below 30 kJ/mol indicating that the adsorption of nitrate anions on the MgZnCoAl-C surface was mainly related to physical interactions, and they could be probably in the form of electrostatic interactions. These calculations also confirmed that the adsorption of nitrate anions was endothermic.

### 3.9 Steric and energetic parameters interpretation, $n$ , $N_m$ , and $Q_{sat}$ :

The steric parameter  $N_m$  describes the necessary effectively occupied receptor sites when the saturation is reached. Fig.13. (b) shows that this parameter varies as a function of the temperature in a non-linear manner. It can be noted that the temperature caused an increment of this density. In fact, there was an increment of the active sites that participate in the adsorption of  $\text{NO}_3^-$ . Note that this density for adsorption system varied with an inverse trend in comparison to the number of nitrate anions per site (i.e., when the parameter  $n$  increased, the corresponding density decreased, and inversely) [39]. on other hand the statistical physics parameters  $n_1$  and

$n_2$  and Analyzing the results of the data fitting given in Table 10 concerning  $n_1$  parameters, it is clear that the values of  $n_i$  ( $i = 1$  and  $2$ ) were greater than unity for the considered temperatures indicating that  $\text{NO}_3^-$  interacted with one type of binding site during the adsorption process. This result indicates that the adsorption process was multi-anionic where each binding site can capture several anions simultaneously. For all temperature results showed that  $n_1 > n_2$ , which indicated that the second type of binding site could have a minor role to remove this anion (74). The parameter  $Q_{\text{sat}}$  represents the adsorbed quantity per gram of studied supports at saturation. According to the statistical physics treatment, the nitrate adsorbed quantity at saturation can be written as  $Q_{\text{sat}} = n N_m$ . Fig.13 (C) shows the variation of the adsorbed quantity at saturation related to all investigated adsorbents. It is clear that the adsorbed quantity increase in temperature from 15 to 25 °C caused an increment of the total adsorbed quantity of nitrate anions thus indicating an endothermic adsorption. Thermal agitation contributed to activate the surface of MgZnCoAl-C causing that more adsorption sites were available for the nitrate anions binding. However, the adsorption quantities decreased from 25 to 40 °C where an exothermic adsorption was present.

### 3.10 Effect of competitive ions:

The effect of competitive ions, on adsorption of nitrate at varying concentrations is shown in fig 14. Our results show that the presence of these anions considerably reduced nitrate adsorption. Anion exchange selectivity is related to the size of the guest anion and its orientation, the ionic radius and the ionic charge ; According to literature, the affinity order of LDHs for the most common anions is carbonate > phosphate > sulphate > nitrate(69). After calcination, the LDH loses its interlayer water, its interlayer anions and the hydroxyls, giving it an extremely positive charge. Research has shown that the adsorptive tendency of multicharged anions is greater than that of monovalent anions (75)(76). In this way, then, the anion with the highest charge density has the greatest effect on nitrate adsorption onto the MgZnCoAl-C. When the solution contains nitrates together with other anions, they could be incorporated into the interlayers. Memory effect is thought to be the mechanism involved in nitrate removal(10).

## 4. Thermodynamics

### 4.1. Macroscopic thermodynamics calculation:

The results obtained for the Gibbs free energy change  $\Delta G^\circ$  are summarized in Table 12 and show values of -2.18, -2.77, -3.65 and -4.24 kJ/mol for nitrate adsorption onto MgZnCoAl-C at 15, 25, 40 and 50 C respectively. These values confirm the spontaneous, thermodynamic nature of the adsorption. The positive value of  $\Delta S^\circ$  indicates that the randomness of the solid-liquid interface increased during the adsorption process. The positive value of  $\Delta H^\circ$  indicates

the endothermic nature of the adsorption process of the nitrate onto MgZnCoAl-C. Furthermore, the magnitude of  $\Delta H^\circ$  describes the interaction between the adsorbent and the adsorbate. Given that the change in adsorption enthalpy is between  $-20$  to  $40$  kJ/mol for physisorption, and between  $40$  and  $80$  kJ/mol for chemisorption, the values obtained in our study ( $14.81$  kJ/mol) indicate a physisorption process.

#### 4.2. Statistics thermodynamics calculations:

The three thermodynamic quantities namely, entropy, free enthalpy and internal energy can be deduced using the canonical grand ensemble in statistical physics, which characterizes the process of adsorption of  $\text{NO}_3^-$  on LDH.

#### 4.3. Configurational entropy:

Entropy is a very important thermodynamic function which depicts the behavior of the adsorbed molecules at the surface of the adsorbent. As such, it gives an idea about the order and disorder on the adsorbent surface during the adsorption process. It is expressed by the grand canonical partition function  $Z_{gc}$ (77):

The value of the sorption entropy is calculated based on the grand potential  $J$ (78), as follows:

$$J = -K_B T \ln Z_{gc} = E_a - \mu_a Q_a - TS_a \quad (26)$$

$$J = \frac{\partial}{\partial \beta} \ln Z_{gc} - T \cdot S_a \quad (27)$$

$$TS_a = -\partial \ln Z_{gc} / \partial \beta + K_B T \ln Z_{gc} \quad (28)$$

$$J = -K_B T \ln Z_{gc} = -\partial \ln Z_{gc} / \partial \beta - TS_a \quad (29)$$

The entropy is then expressed by:

$$S_a K_B = -\beta \partial \ln Z_{gc} / \partial \beta + \ln Z_{gc} \quad (30)$$

Subsequently, the sorption entropy  $S_a$  can be expressed as:

$$\frac{S}{K_B} = N_{S1} \left[ \ln \left( 1 + \left( \frac{C_e}{C_1} \right)^{n_{m1}} \right) + \frac{n_{m1} \ln \left( \frac{C_1}{C_e} \right)}{1 + \left( \frac{C_1}{C_e} \right)^{n_{m1}}} \right] + N_{S2} \left[ \ln \left( 1 + \left( \frac{C_e}{C_2} \right)^{n_{m2}} \right) + \frac{n_{m2} \ln \left( \frac{C_2}{C_e} \right)}{1 + \left( \frac{C_2}{C_e} \right)^{n_{m2}}} \right] \quad (31)$$

The profile of the entropy evolution as function of the water activity is given in Fig. 15.

Fig.15, shows that the entropy increases with the increasing value of  $C_e$  up to a certain value corresponding to the  $S_{\max}$  values obtained and then decreases after these particular points

for the three temperatures. At first, the disorder on the surface of the adsorbent increases because the solute has several chances to find an empty receptor site. After these distinctive points, the probability that the adsorbate will find an adsorption site decreases because the surface tends to saturate in order to become ordered. The  $S_{\max}$  reflect the maximum disorders at the level of the monolayer (79). It can also be noted that the peaks corresponding to  $C_e$  for  $S_{\max}$  describe the adsorbent-adsorbent interaction before the disorder value changes.

From Fig. 15, the entropy shows a maximum at particular concentrations 13.24mg/L, 45.8mg/L and 102.48mg/L, for all temperatures. In fact, entropy increases rapidly with concentrations below 120mg/L. This is explained by the increase in the disorder on the adsorbent surface because the adsorbed solute molecule has more or more chance of finding a free receptor site in order to attach, so the entropy reaches the value almost equal to 72% of saturation or adsorption equilibrium for the temperature 25 °C while for the temperature of 40 °C the maximum entropy is reached only after the concentration at equilibrium equal to  $C_e = 102.48 \text{ mg / L}$  which means that the temperature increases the probability for molecules to find a free site. Beyond the max values, the entropy decreases more rapidly for the case of the adsorption carried out at 25 °C compared to that of 40 °C, since the possibilities of finding an empty site decrease more and more when the saturation of the layer is almost reached, or the limitation of the degree of freedom because the nitrate ion can be anchored by two oxygen at the same time.

#### 4.4. Free sorption enthalpy

The free enthalpy determines the spontaneity of an adsorption process (given system is spontaneous or not) (80). The evolution of this potential function was investigated by calculating its expression according to the double layer model with two energies. The free enthalpy to the model of the double layer with two energies is given in table 4.

Fig.16 represents the evolution of the free enthalpy as a function of the concentration of nitrate in solution for the system studied at three different temperatures. However, the free energy values for the three temperatures are negative thus showing the spontaneity of the adsorption reaction(81). The increase in free enthalpy for the temperature of 40 °C compared with the other two temperatures shows an increase in the feasibility of adsorption. The increases in the adsorption capacity of  $\text{NO}_3^-$  for the three temperatures are more or less quite close. However the knowledge of this free energy is important to know the mechanism of the adsorption (78).

In common, any reaction whose variation in free sorption enthalpy  $\Delta G$  is negative should be favorable. As a consequence, its investigation is vital to interpret the physical sorption mechanism. It can be expressed by the expression cited in the table 4.

#### 4.5. Internal sorption energy:

Internal energy is a thermodynamic parameter which specifies the nature of the adsorption phenomenon. Its expression after using the chemical potential and the partition function is given in table 4 (39)(79).

$$E_{int} = K_B T \left[ N_{S1} \frac{\ln\left(\frac{c}{z_v}\right) + n_{m1} \ln\left(\frac{c_1}{c}\right)}{1 + \left(\frac{c_1}{c}\right)n_{m1}} + N_{S2} \frac{\ln\left(\frac{c}{z_v}\right) + n_{m2} \ln\left(\frac{c_2}{c}\right)}{1 + \left(\frac{c_2}{c}\right)n_{m2}} \right] \quad (32)$$

We emphasize that the internal sorption energy is generally negative. This physical quantity is stable for the three temperatures (15-40 °C) for concentrations above 200 (Ce = 200 mg/L) after saturation of the nitrate molecules adsorbed on the adsorbent material. Note also that the internal energy increases with the increase in temperature or this could be explained by the increase in thermal collision. Fig.17, shows the evolution of the internal energy at 15 °C, 25 °C and 40°C.

#### 5. Adsorption mechanism

The adsorption mechanism of nitrate ions on MgZnCoAl-C is essential to understand the removal of nitrates from an aqueous medium. Thus the reconstruction of MgZnCoAl-CO<sub>3</sub> called "memory effect" is considered as one of the adsorption mechanisms when LDH-C adsorbs nitrates. Moreover, it was found from the XRD diagrams (Fig.2), that LDH-C had no peaks characteristic of LDHs. *The peaks at 43.4° and 63.7°, (Fig.2b) are attributed to metal oxides.* Thus, after adsorption of the nitrate ions, the following peaks (003, 006), (Fig 2c) reappeared; which confirms that the nitrate is indeed adsorbed on LDH [82].

The experimental isotherm points obtained are similar to monolayer adsorption (type I) encountered in the case of microporous adsorbents. The rapid increase in the quantity adsorbed for low concentrations corresponds to the filling of all the volumes of the micropores available up to saturation. Other studies have shown that multilayer adsorption can give the same appearance [83].

Additionally, MgZnCoAl-C recovered its original stratified structure after adsorption of nitrate ions. This is visible through the intensity of the peak at about 1380 cm<sup>-1</sup> which has

become less strong after the absorption of the nitrate ion. This is obtained after rehydration followed by structural reconstruction in the presence of adsorbed nitrate ions. Thus, we note that the peaks at 1500 and 1104  $\text{cm}^{-1}$  reappeared again after adsorption of the nitrate ion; which indicated the adsorption of nitrate [32].

The Sips model predicts the heterogeneity of adsorbate-adsorbent interaction. It is only a combination of the Langmuir and Freundlich models, thus, at a high concentration of adsorbate, the Sips model gives the monolayer Langmuir model. While, if the adsorbate concentration is low, the Sips model is reduced to the Freundlich model.

The surface of the material therefore contains several adsorption sites with different energies available and each site can be suitable for a single adsorbed molecule. However, the adsorbate-adsorbent interaction sites are independent and therefore have different affinities. In this case, the Freundlich model can be used for multilayer adsorption where the adsorption energy and affinities are not uniformly distributed over a heterogeneous material surface. Therefore, sites that have high energy will be charged first, and then the weakest will be occupied afterward at the end of the adsorption process [84].

Statistical models generally help to interpret the mechanism at the microscopic scale of adsorbent-adsorbate interaction. Thus, based on the statistical models, we notice that the monolayer model with two active sites having different binding energies confirms that the Sips model describes well the adsorption mechanism. The number “ $n_i$ ” being greater than unity confirms that this adsorption takes place with different adsorption sites and that the nitrate molecules do not adsorb in a parallel way but rather in a non-parallel way where several nitrate ions can be anchored with a single site simultaneously. This is referred to as multi-anion adsorption. LDH has a wide band of positive charges on its surface which favors electrostatic adsorption with the negative charges of nitrates. The enthalpy of adsorption given by the monolayer model at two different energies confirms clearly a physical adsorption (electrostatic type). The  $\Delta E_1$  and  $\Delta E_2$  energy values are less than 40 kJ/mol indicating that the adsorption of nitrate ions on the LDH surface is mainly linked to physical interactions. Thus, the variation of the adsorption energies confirms that the two adsorption sites have effectively participated in the elimination of nitrates. Finally, we can see that the statistical model is complementary to other classic models and has predicted in a satisfactory way the mechanism of interaction between materials and nitrate ions.

## 6. Conclusion

In conclusion, a new layered double hydroxide composed of four metals, Mg–Zn–Co–Al-LDH was successfully synthesized using the co-precipitation method at constant pH. It was demonstrated that LDH was an efficient adsorbent for the nitrate removal. The textural properties obtained for LDH and CLDH demonstrated that the calcination increased the specific surface area by the release of water and carbon dioxide forming larger pores and free surface. Our research shows that a maximum nitrate adsorption capacity of 72.73mg/g was obtained when the CLDH sample was heated to a temperature of 25°C. From the four kinetic models tested, the Pseudo-Second Order model best fitted the experimental data, indicating that the physical interactions between the adsorbate and the surface of the adsorbent dominated the adsorption process. The intraparticle diffusion model, used to ascertain the mechanism of the adsorption process, showed not only intraparticle diffusion, but also an external diffusion of nitrate molecules onto the surface of the LDH. Of the four adsorption isotherms studied, the Sips model represented best the equilibrium results, while a monolayer adsorption model from Statistical physics with two binding sites was used retrieve supplemental information about the nitrate anions adsorption mechanism, The results suggested a multimolecular process and the physical adsorption of nitrate onto the MgZnCoAl-C. Thermodynamic analysis showed that the adsorption was spontaneous and endothermic in nature. Our study has shown that MgZnCoAl-C can effectively be used to removal nitrate and reduce their concentration to acceptable levels. Subsequently, this process can be employed as the first step in eliminating nitrates from both surface and groundwater in an attempt to meet authorized levels.

### **Acknowledgments**

The authors would like to thank the MESRS and DGRSDT (Ministère de l'Enseignement Supérieur et de la Recherche Scientifique et la Direction Générale de la Recherche Scientifique et du Développement Technologique- Algérie) for their Financial support.

## References

1. Bakhti A, Ouali MS. Sorption des ions chromate sur une hydrotalcite de synthèse calcinée. *Water QualRes J Can.* 2005 May;40(2):177–83.
2. Grégoire B. Relation Composition-Structure des Hydroxydes Doubles Lamellaires: Effets de la charge du feuillet et de la nature de l'anion interfoliaire [PhD Thesis]. Université de Lorraine; 2012.
3. Charradi K, Gondran C, Moutet J-C, Forano C, Vanessa P, Christine M. Contribution des argiles ferrifères à l'élaboration de biocapteurs ampérométriques: Etude de l'interaction de l'Hémoglobine avec des Argiles et des Hydroxydes Doubles Lamellaires. [PhD Thesis]. 2010.
4. Drici N. Hydroxydes doubles lamellaires, synthèse, caractérisation et propriétés [PhD Thesis]. 2015.
5. Halajnia A, Oustan S, Najafi N, Khataee AR, Lakzian A. The adsorption characteristics of nitrate on Mg–Fe and Mg–Al layered double hydroxides in a simulated soil solution. *Applied Clay Science.* 2012;70:28–36.
6. Géraud E. Elaboration et caractérisation de matrices hydroxydes doubles lamellaires macroporeuses [PhD Thesis]. 2006.
7. Goh K-H, Lim T-T, Dong Z. Application of layered double hydroxides for removal of oxyanions: a review. *Water research.* 2008;42(6–7):1343–68.
8. Hafshejani LD, Hooshmand A, Naseri AA, Mohammadi AS, Abbasi F, Bhatnagar A. Removal of nitrate from aqueous solution by modified sugarcane bagasse biochar. *Ecological Engineering.* 2016;95:101–11.

9. Yang QZ, Sun DJ, Zhang CG, Wang XJ, Zhao WA. Synthesis and characterization of polyoxyethylene sulfate intercalated Mg- Al- nitrate layered double hydroxide. *Langmuir*. 2003;19(14):5570–4.
10. Socías-Viciano MM, Ureña-Amate MD, González-Pradas E, García-Cortés MJ, López-Teruel C. Nitrate removal by calcined hydrotalcite-type compounds. *Clays and clay minerals*. 2008;56(1):2–9.
11. Milagres JL, Bellato CR, Vieira RS, Ferreira SO, Reis C. Preparation and evaluation of the Ca-Al layered double hydroxide for removal of copper (II), nickel (II), zinc (II), chromium (VI) and phosphate from aqueous solutions. *Journal of environmental chemical engineering*. 2017;5(6):5469–80.
12. Hatami H, Fotovat A, Halajnia A. Comparison of adsorption and desorption of phosphate on synthesized Zn-Al LDH by two methods in a simulated soil solution. *Applied Clay Science*. 2018;152:333–41.
13. Luengo CV, Volpe MA, Avena MJ. High sorption of phosphate on Mg-Al layered double hydroxides: Kinetics and equilibrium. *Journal of environmental chemical engineering*. 2017;5(5):4656–62.
14. Lahkale R, Sadik R, Sabbar E. Elimination du chrome trivalent d'un rejet de tannerie par un hydroxyde double lamellairecalciné (Removal of trivalent chromium from tannery effluent by calcined layered double hydroxide). *J Mater Environ Sci*. 2014;5(S2):2403–8.
15. Hsu LC, Wang SL, Tzou YM, Lin CF, Chen JH. The removal and recovery of Cr (VI) by Li/Al layered double hydroxide (LDH). *Journal of Hazardous Materials*. 2007;142(1–2):242–9.
16. Inacio J, Taviot-Gueho C, Forano C, Besse JP. Adsorption of MCPA pesticide by MgAl-layered double hydroxides. *Applied Clay Science*. 2001;18(5–6):255–64.

17. Liu A, Ming J, Ankumah RO. Nitrate contamination in private wells in rural Alabama, United States. *Science of the total environment*. 2005;346(1–3):112–20.
18. Bhatnagar A, Kumar E, Sillanpää M. Nitrate removal from water by nano-alumina: Characterization and sorption studies. *Chemical Engineering Journal*. 2010;163(3):317–23.
19. Berber MR, Hafez IH, Minagawa K, Mori T. A sustained controlled release formulation of soil nitrogen based on nitrate-layered double hydroxide nanoparticle material. *Journal of soils and sediments*. 2014;14(1):60–6.
20. DES MATÉRIAUX PENP. ADSORPTION ET DÉSORPTION D'IONS PHOSPHATE ET NITRATE PAR DES MATÉRIAUX MÉSOPOREUX À BASE DE SILICE FONCTIONNALISÉS AVEC DES GROUPEMENTS AMMONIUM. 2008;
21. Sellaoui L, Guedidi H, Knani S, Reinert L, Duclaux L, Lamine AB. Application of statistical physics formalism to the modeling of adsorption isotherms of ibuprofen on activated carbon. *Fluid phase equilibria*. 2015;387:103–10.
22. Sellaoui L, Soetaredjo FE, Ismadji S, Lima ÉC, Dotto GL, Lamine AB, et al. New insights into single-compound and binary adsorption of copper and lead ions on a treated sea mango shell: experimental and theoretical studies. *Physical Chemistry Chemical Physics*. 2017;19(38):25927–37.
23. Sellaoui L, Dotto GL, Peres EC, Benguerba Y, Lima ÉC, Lamine AB, et al. New insights into the adsorption of crystal violet dye on functionalized multi-walled carbon nanotubes: experiments, statistical physics and COSMO–RS models application. *Journal of Molecular Liquids*. 2017;248:890–7.
24. Reichle WT. Synthesis of anionic clay minerals (mixed metal hydroxides, hydrotalcite). *Solid State Ionics*. 1986;22(1):135–41.

25. Benhouria A, Islam MA, Zaghouane-Boudiaf H, Boutahala M, Hameed BH. Calcium alginate–bentonite–activated carbon composite beads as highly effective adsorbent for methylene blue. *Chemical engineering journal*. 2015;270:621–30.
26. Rodier J, Geoffroy C, Rodi L. L'analyse de l'eau: eaux naturelles, eaux résiduaires, eau de mer: chimie, physico-chimie, bactériologie, biologie. Dunod Paris; 1984.
27. Lagergren SK. About the theory of so-called adsorption of soluble substances. *Sven VetenskapsakadHandlingar*. 1898;24:1–39.
28. Ho Y-S, McKay G. Pseudo-second order model for sorption processes. *Process biochemistry*. 1999;34(5):451–65.
29. Juang R-S, Chen M-L. Application of the Elovich equation to the kinetics of metal sorption with solvent-impregnated resins. *Industrial & Engineering Chemistry Research*. 1997;36(3):813–20.
30. Weber Jr WJ, Morris JC. Kinetics of adsorption on carbon from solution. *Journal of the sanitary engineering division*. 1963;89(2):31–59.
31. Chabani M, Amrane A, Bensmaili A. Kinetic modelling of the adsorption of nitrates by ion exchange resin. *Chemical Engineering Journal*. 2006;125(2):111–7.
32. Islam M, Patel R. Physicochemical characterization and adsorption behavior of Ca/Al chloride hydrotalcite-like compound towards removal of nitrate. *Journal of hazardous materials*. 2011;190(1–3):659–68.
33. Mathias PM, Kumar R, Moyer JD, Schork JM, Srinivasan SR, Auvil SR, et al. Correlation of multicomponent gas adsorption by the dual-site Langmuir model. Application to nitrogen/oxygen adsorption on 5A-zeolite. *Industrial & engineering chemistry research*. 1996;35(7):2477–83.
34. Freundlich HMF. Over the adsorption in solution. *J Phys Chem*. 1906;57(385471):1100–7.

35. Sips R. On the structure of a catalyst surface. *The journal of chemical physics*. 1948;16(5):490–5.
36. Peterson DL, Redlich O. A useful adsorption isotherm. *J Phys Chem*. 1959;63:1024–1024.
37. Nakhli A, Mbouga MGN, Bergaoui M, Khalfaoui M, Cretin M, Huguet P. Non-linear analysis in estimating model parameters for thymol adsorption onto hydroxyiron-clays. *Journal of Molecular Liquids*. 2017;244:201–10.
38. Khalfaoui M, El Ghali A, Aguir C, Mohamed Z, Baouab MHV, Lamine AB. Study on adsorption of herbicide onto functionalized cellulose extracted from *Juncus acutus* L. plant: Experimental results and theoretical modeling. *Industrial Crops and Products*. 2015;67:169–78.
39. Yazidi A, Sellaoui L, Dotto GL, Bonilla-Petriciolet A, Fröhlich AC, Lamine AB. Monolayer and multilayer adsorption of pharmaceuticals on activated carbon: application of advanced statistical physics models. *Journal of Molecular Liquids*. 2019;283:276–86.
40. Sellaoui L, Ali J, Badawi M, Bonilla-Petriciolet A, Chen Z. Understanding the adsorption mechanism of  $\text{Ag}^+$  and  $\text{Hg}^{2+}$  on functionalized layered double hydroxide via statistical physics modeling. *Applied Clay Science*. 2020;198:105828.
41. Sellaoui L, Franco D, Ghalla H, Georgin J, Netto MS, Dotto GL, et al. Insights of the adsorption mechanism of methylene blue on brazilian berries seeds: Experiments, phenomenological modelling and DFT calculations. *Chemical Engineering Journal*. 2020;394:125011.
42. Alyousef H, Yahia MB, Aouaini F. Statistical physics modeling of water vapor adsorption isotherm into kernels of dates: Experiments, microscopic interpretation and thermodynamic functions evaluation. *Arabian Journal of Chemistry*. 2020;13(3):4691–702.
43. Milonjić SK. A consideration of the correct calculation of thermodynamic parameters of adsorption. *Journal of the Serbian chemical society*. 2007;72(12):1363–7.

44. Pesic L, Salipurovic S, Markovic V, Vucelic D, Kagunya W, Jones W. Thermal characteristics of a synthetic hydrotalcite-like material. *Journal of Materials Chemistry*. 1992;2(10):1069–73.
45. Fatima K, Karima E, Mayouf S, Abdallah L, Nourredine B. Séminaire Eau et Environnement (SEE2011). 2011;5.
46. Zhang L, Liu J, Xiao H, Liu D, Qin Y, Wu H, et al. Preparation and properties of mixed metal oxides based layered double hydroxide as anode materials for dye-sensitized solar cell. *Chemical Engineering Journal*. 2014;250:1–5.
47. Wan D, Liu H, Liu R, Qu J, Li S, Zhang J. Adsorption of nitrate and nitrite from aqueous solution onto calcined (Mg–Al) hydrotalcite of different Mg/Al ratio. *Chemical Engineering Journal*. 2012;195:241–7.
48. Pérez-Ramírez J, Mul G, Kapteijn F, Moulijn JA. On the stability of the thermally decomposed Co–Al hydrotalcite against retrotopotactic transformation. *Materials research bulletin*. 2001;36(10):1767–75.
49. Eshaq G, Rabie AM, Bakr AA, Mady AH, ElMetwally AE. Cr (VI) adsorption from aqueous solutions onto Mg–Zn–Al LDH and its corresponding oxide. *Desalination and Water Treatment*. 2016;57(43):20377–87.
50. Yang W, Kim Y, Liu PK, Sahimi M, Tsotsis TT. A study by in situ techniques of the thermal evolution of the structure of a Mg–Al–CO<sub>3</sub> layered double hydroxide. *Chemical Engineering Science*. 2002;57(15):2945–53.
51. Harizi I, Chebli D, Bouguettoucha A, Rohani S, Amrane A. A new Mg–Al–Cu–Fe-LDH composite to enhance the adsorption of acid red 66 dye: Characterization, kinetics and isotherm analysis. *Arabian Journal for Science and Engineering*. 2019;44(6):5245–61.

52. Lv L, He J, Wei M, Evans DG, Duan X. Factors influencing the removal of fluoride from aqueous solution by calcined Mg–Al–CO<sub>3</sub> layered double hydroxides. *Journal of Hazardous Materials*. 2006;133(1–3):119–28.
53. Karami Z, Jouyandeh M, Ali JA, Ganjali MR, Aghazadeh M, Paran SMR, et al. Epoxy/layered double hydroxide (LDH) nanocomposites: Synthesis, characterization, and Excellent cure feature of nitrate anion intercalated Zn-Al LDH. *Progress in Organic Coatings*. 2019;136:105218.
54. Sing KS, Everett DH, Haul RAW, Moscou L, Pierotti RA, Rouquerol J, et al. Reporting physisorption data for gas/solid systems with special reference to the determination of surface area and porosity (Recommendations 1984). *Pure appl chem*. 1985;57(4):603–19.
55. Thommes M, Kaneko K, Neimark AV, Olivier JP, Rodriguez-Reinoso F, Rouquerol J, et al. Physisorption of gases, with special reference to the evaluation of surface area and pore size distribution (IUPAC Technical Report). *Pure and applied chemistry*. 2015;87(9–10):1051–69.
56. Zhou J, Yang S, Yu J, Shu Z. Novel hollow microspheres of hierarchical zinc–aluminum layered double hydroxides and their enhanced adsorption capacity for phosphate in water. *Journal of hazardous materials*. 2011;192(3):1114–21.
57. Bouarouria K, Naceura MW, Haninib S, Soukanea S, Laidib M, Drouichec N. Adsorption of humic acid from seawater on organo Mg–Fe-layered double hydroxides: isotherm, kinetic modeling, and ionic strength. *DESALINATION AND WATER TREATMENT*. 2020;195:114–27.
58. Zaghouane-Boudiaf H, Boutahala M, Arab L. Removal of methyl orange from aqueous solution by uncalcined and calcined MgNiAl layered double hydroxides (LDHs). *Chemical Engineering Journal*. 2012;187:142–9.

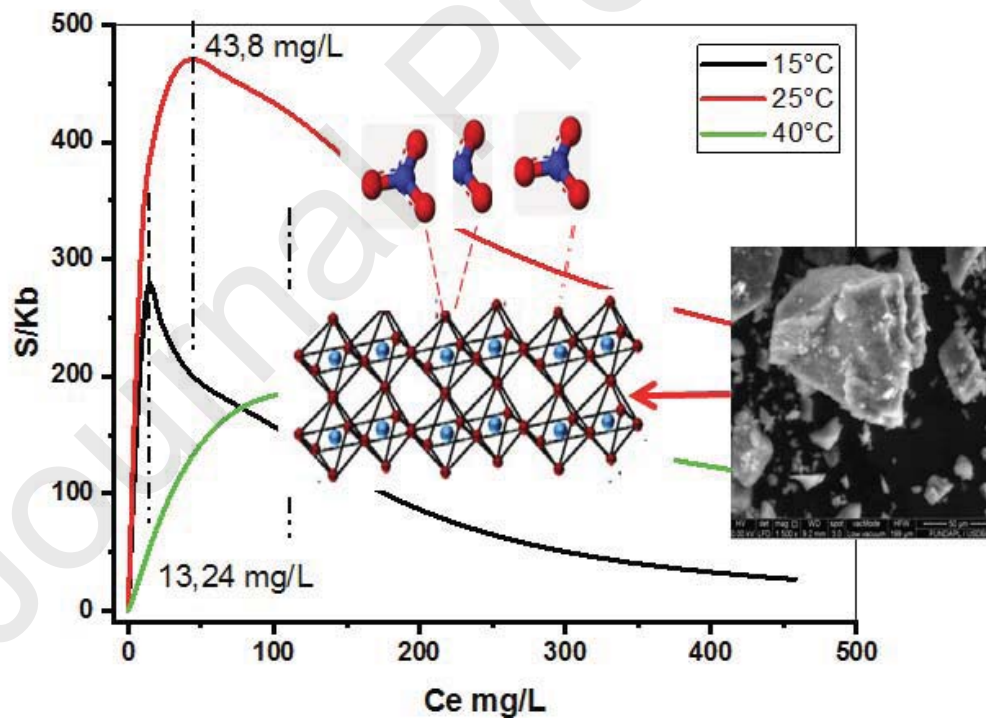
59. Lin Y, Fang Q, Chen B. Perchlorate uptake and molecular mechanisms by magnesium/aluminum carbonate layered double hydroxides and the calcined layered double hydroxides. *Chemical Engineering Journal*. 2014;237:38–46.
60. Mohammadi M, MohammadiTorkashvand A, Biparva P, Esfandiari M. Synthesis ratios of Mg-Al and Zn-Al layered double hydroxides efficiency and selectivity in nitrate removal from solution. *Global Journal of Environmental Science and Management*. 2019;5(4):485–500.
61. Chebli D, Bouguettoucha A, Reffas A, Tiar C, Boutahala M, Gulyas H, et al. Removal of the anionic dye Biebrich scarlet from water by adsorption to calcined and non-calcined Mg–Al layered double hydroxides. *Desalination and Water Treatment*. 2016;57(46):22061–73.
62. Islam M, Patel R. Synthesis and physicochemical characterization of Zn/Al chloride layered double hydroxide and evaluation of its nitrate removal efficiency. *Desalination*. 2010 Jun;256(1–3):120–8.
63. Mohammadi M, Bahmanyar MA, Sadeghzadeh F, Biparva P. Synthesis of Mg/Al layered double hydroxide (LDH) nanoplates for efficient removal of nitarate from aqueous solutions. *Journal of Fundamental and Applied Sciences*. 2016;8(2):1058–71.
64. Tiar C, Boutahala M, Benhouria A, Zaghouane-Boudiaf H. Synthesis and physicochemical characterization of ZnMgNiAl-CO<sub>3</sub>-layered double hydroxide and evaluation of its sodium dodecylbenzenesulfonate removal efficiency. *Desalination and Water Treatment*. 2016;57(28):13132–43.
65. Santos LC, da Silva AF, dos Santos Lins PV, da Silva Duarte JL, Ide AH, Meili L. Mg-Fe layered double hydroxide with chloride intercalated: synthesis, characterization and application for efficient nitrate removal. *Environmental Science and Pollution Research*. 2020;27(6):5890–900.

66. Kadirvelu K, Faur-Brasquet C, Cloirec PL. Removal of Cu (II), Pb (II), and Ni (II) by adsorption onto activated carbon cloths. *Langmuir*. 2000;16(22):8404–9.
67. Giles CH, MacEwan TH, Nakhwa SN, Smith D. 786. Studies in adsorption. Part XI. A system of classification of solution adsorption isotherms, and its use in diagnosis of adsorption mechanisms and in measurement of specific surface areas of solids. *Journal of the Chemical Society (Resumed)*. 1960;3973–93.
68. Maia GS, de Andrade JR, da Silva MG, Vieira MG. Adsorption of diclofenac sodium onto commercial organoclay: kinetic, equilibrium and thermodynamic study. *Powder technology*. 2019;345:140–50.
69. Ivánová D, Albert P, Kavuličová J. Nitrate removal from model aqueous solutions and real water by calcined Mg/Al layered double hydroxides. *Applied Clay Science*. 2018;152:65–72.
70. Hosni K, Srasra E. Nitrate adsorption from aqueous solution by M II-Al-CO<sub>3</sub> layered double hydroxide. *Inorganic Materials*. 2008;44(7):742–9.
71. Li Z, Hanafy H, Zhang L, Sellaoui L, Netto MS, Oliveira ML, et al. Adsorption of congo red and methylene blue dyes on an ashitaba waste and a walnut shell-based activated carbon from aqueous solutions: Experiments, characterization and physical interpretations. *Chemical Engineering Journal*. 2020;388:124263.
72. Li Z, Sellaoui L, Dotto GL, Bonilla-Petriciolet A, Lamine AB. Understanding the adsorption mechanism of phenol and 2-nitrophenol on a biopolymer-based biochar in single and binary systems via advanced modeling analysis. *Chemical Engineering Journal*. 2019;371:1–6.
73. Dhaouadi F, Sellaoui L, Taamalli S, Louis F, El Bakali A, Junior TRSC, et al. A statistical physics analysis of the adsorption of Fe<sup>3+</sup>, Al<sup>3+</sup> and Cu<sup>2+</sup> heavy metals on chitosan films

- via homogeneous and heterogeneous monolayer models. *Journal of Molecular Liquids*. 2021;343:117617.
74. Dhaouadi F, Sellaoui L, Badawi M, Reynel-Ávila HE, Mendoza-Castillo DI, Jaime-Leal JE, et al. Statistical physics interpretation of the adsorption mechanism of  $Pb^{2+}$ ,  $Cd^{2+}$  and  $Ni^{2+}$  on chicken feathers. *Journal of Molecular Liquids*. 2020 Dec;319:114168.
75. Das J, Patra BS, Baliarsingh N, Parida KM. Adsorption of phosphate by layered double hydroxides in aqueous solutions. *Applied Clay Science*. 2006;32(3–4):252–60.
76. Tezuka S, Chitrakar R, Sonoda A, Ooi K, Tomida T. Studies on selective adsorbents for oxo-anions. Nitrate ion-exchange properties of layered double hydroxides with different metal atoms. *Green Chemistry*. 2004;6(2):104–9.
77. Khalfaoui M, Nakhli A, Knani S, Baouab HV, Ben Lamine A. On the statistical physics modeling of dye adsorption onto anionized nylon: consequent new interpretations. *Journal of applied polymer science*. 2012;125(2):1091–102.
78. Couture L, Zitoun R. *Statistical physics; Physique statistique*. 1992;
79. Aouaini F, Knani S, Yahia MB, Lamine AB. Statistical physics studies of multilayer adsorption isotherm in food materials and pore size distribution. *Physica A: Statistical Mechanics and its Applications*. 2015;432:373–90.
80. Mohamed B, Qingyu Z, Moggridge GD, Abdelmottaleb BL. New insight in adsorption of pyridine on the two modified adsorbents types MN200 and MN500 by means of grand canonical ensemble. *Journal of Molecular Liquids*. 2018;263:413–21.
81. Zhou X, Yi H, Tang X, Deng H, Liu H. Thermodynamics for the adsorption of  $SO_2$ ,  $NO$  and  $CO_2$  from flue gas on activated carbon fiber. *Chemical Engineering Journal*. 2012;200:399–404.
82. Ferreira OP, De Moraes SG, Duran N, Cornejo L, Alves OL. Evaluation of boron removal from water by hydrotalcite-like compounds. *Chemosphere*. 2006;62(1):80–8.

83. Knani S. Contribution à l'étude de la gustation des molécules sucrées à travers un processus d'adsorption. Modélisation par la physique statistique. Thèse de Doctorat. 2007;
84. Gast AP, Adamson AW. Physical chemistry of surfaces. Wiley New York; 1997.

### Graphical Abstract



### Highlights

High adsorption efficiency of nitrate ions in aqueous solution

Statistical physics models can explain the mechanism of adsorption

Four-element LDH provides multi-energy adsorption sites

LDH synthesized by the coprecipitation method provides good crystallinity

ELHACHEMI Mounira



CHEMAT-DJENNI Zoubida



CHEBLI Derradji



BOUGUETTOUCHA Abdallah



AMRANE Abdeltif



### **Biography of Mrs. ELHACHEMI Mounira**

Elhachemi Mounira is currently a PhD student of process engineering at the University of Blida in Algeria. She is interested in materials engineering and treatment water. Her doctoral work explores the development of new materials which have a layered double hydroxide base, with the aim of eliminating micro pollutants and treatment of sea water and brackish water. She is a co-author of four master grade students in materials engineering. She has participated in two national workshops in (bibliography and writing; development of materials), she has three international communications and two national communications in several filed like: environmental engineering; process engineering and materials chemistry.

### **Biography of Professor CHEMAT-DJENNI Zoubida**

Zoubida CHEMAT-DJENNI (55 years old), is a Professor and heading a team "Green chemistry and Processes" at the Research Laboratory in Functional Analysis of Chemical Processes (LAFPC) at the University Blida1 Algeria. With a process engineering background, she obtained in 2008 a PhD in Chemical Engineering, with a major in Petrochemistry, then a habilitation to supervise research teams in 2014. Her research focuses on the characterization of natural and synthetic clays and their application as adsorbents mainly for the retention of organic and inorganic pollutants as well as other applications for the purification of herbal extracts. In addition, she has developed unique expertise on using those metallic organic frameworks (MOFs) as catalysts for the hemisynthesis and chemical synthesis with an aim to propose them as encapsulating agents in pharmaceutical formulations.

She is currently supervising 6 PhD candidates and has a track record of more than 12 peer reviewed publications and others in press, participation to 18 international conferences and collaborated in 6 PRFU research projects.

### **Biography of Professor Chebli Derradji**

Pr. Chebli Derradji began his professional career as engineer in cement and drilling fluid at the national well service company ENSP, Hassi Messaoud, then head of aerosol production at ASMIDAL company, Batna and finally head of laboratory service at the station drinking water treatment plant in Ain Zada , Setif, Algeria. Currently CHEBLI Derradji is a Professor at the University of Sétif 1. For about a few years his research has been entirely devoted, above all, to the development of combined Adsorption/Photocatalysis, Photocatalysis /Biological treatment processes for the elimination of organic pollutants in wastewater effluents at the chemical process engineering laboratory, LGPC within the chemistry and environmental process engineering team, CIPE. He has supervised 4 doctoral theses as thesis director and 3 are in progress; he has also co-directed 2 doctoral theses and 2 co-supervised theses are in progress. He has been involved in several projects as a manager or participant, as well as in an international collaboration (France). He has published over 30 international articles and others in press.

### **Biography of Professor BOUGUETTOUCHA Abdallah**

BOUGUETTOUCHA Abdallah, Professor, graduated from high school at the age of 18 in 1988 Then, he obtained diplomas -Engineering (1993); Magister (1998) at the University of Sétif-1 Algeria the doctorate degree in chemistry from the University of Rennes -1 in 2009. France. He joined the University of Sétif-1 in 2000 as an assistant professor, then as an associate professor and today he has the rank of professor. The research area covers separation processes, citing among others, the elimination of liquid effluents and photocatalysis. He has supervised 03 doctoral theses as thesis director and 4 are in progress. he has contributed to more than 35 papers in renowned international journals.

### **Biography of Professor AMRANE Abdeltif**

AMRANE Abdeltif (56 years old) Professor – Exceptional class, UMR CNRS 6226 ISCR, University of Rennes 1. (Google Scholar: h-index: 54; citations: 11325 // Scopus: hindex: 44; citations: 7872). 1998: Thesis Director Enabling Degree (Univ. Rennes 1) / 1991: PhD in Chemistry (Univ. Rennes 1) / 1988: Master (DEA) in Chemistry (Univ. Rennes 1) / 1987: Chemical Engineering Degree (USTHB – Algeria). Since approximately 15 years his research is entirely devoted to the development of combined processes for the removal of organic pollutants in effluent wastewater and gaseous emissions within the CIP team. He has managed

16 PhD theses as thesis director and 2 are in progress; he has also comanged 24 PhD theses and 4 co-managements theses are in progress. He has been involved as a manager or a participant in several national and international projects, as well in international collaborations (Algeria, Belgium, Hungary, Iran, Lebanon, Mexico, Morocco, Poland, Portugal, Romania, Spain, Tunisia...). He has published more than 400 international papers including 15 papers in press. He is the co-Editor of three books (Elsevier). He has also published 12 chapter books and has about 130 international and 20 national oral communications.

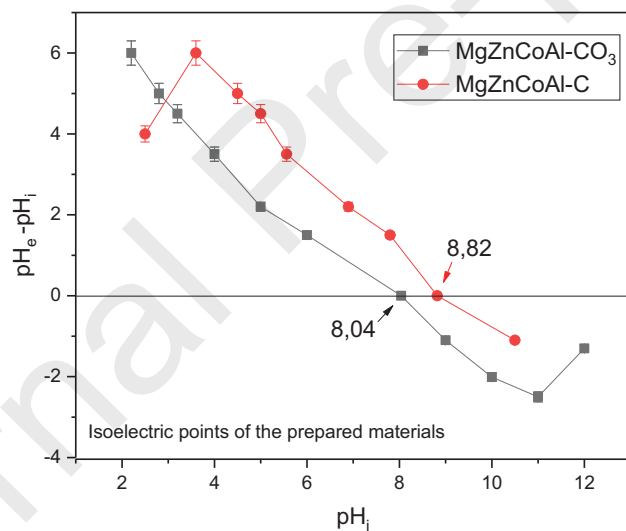


**Fig.1.** Isoelectric points of the prepared materials.

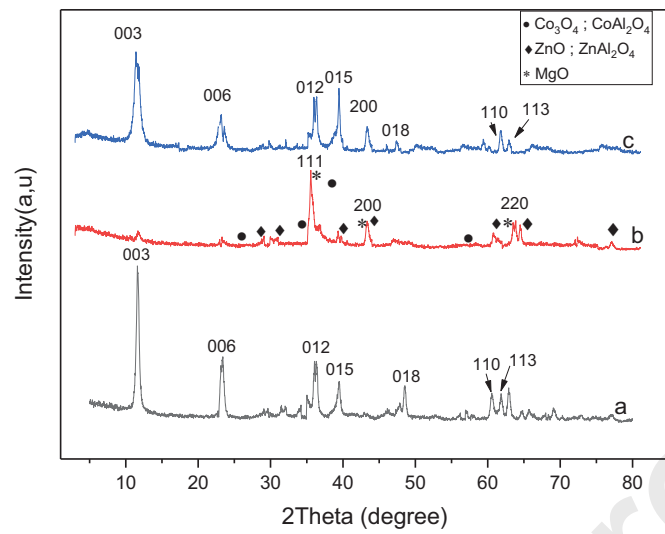


**Fig.2.** XRD patterns of (a) MgZnCoAl-CO<sub>3</sub>; (b) MgZnCoAl-C; (c) MgZnCoAl-NO<sub>3</sub><sup>-</sup>

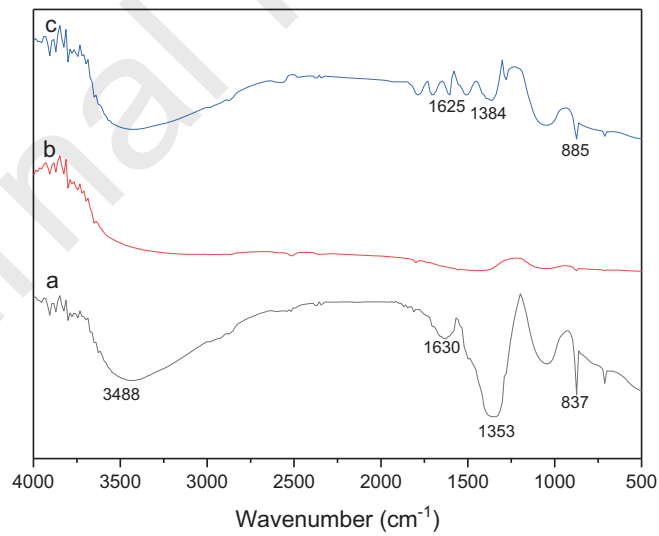


**Fig.3.** FTIR spectra for (a) MgZnCoAl-CO<sub>3</sub>, (b) MgZnCoAl-C, (c) MgZnCoAl-NO<sub>3</sub>

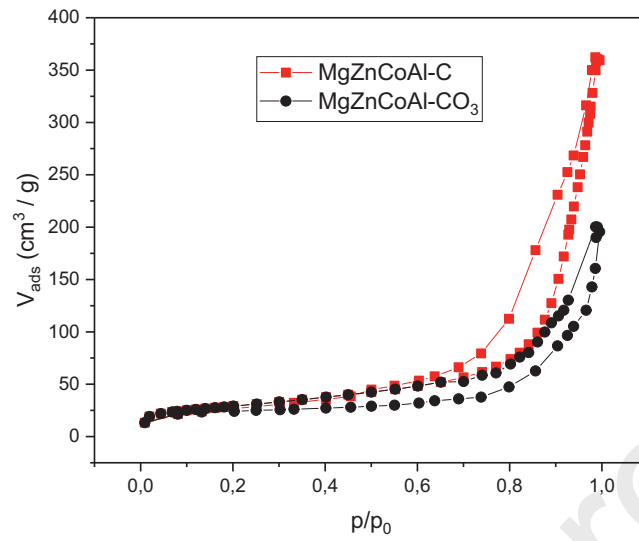


Fig.4. Adsorption/desorption isotherms of MgZnCoAl-CO<sub>3</sub> and MgZnCoAl-C.

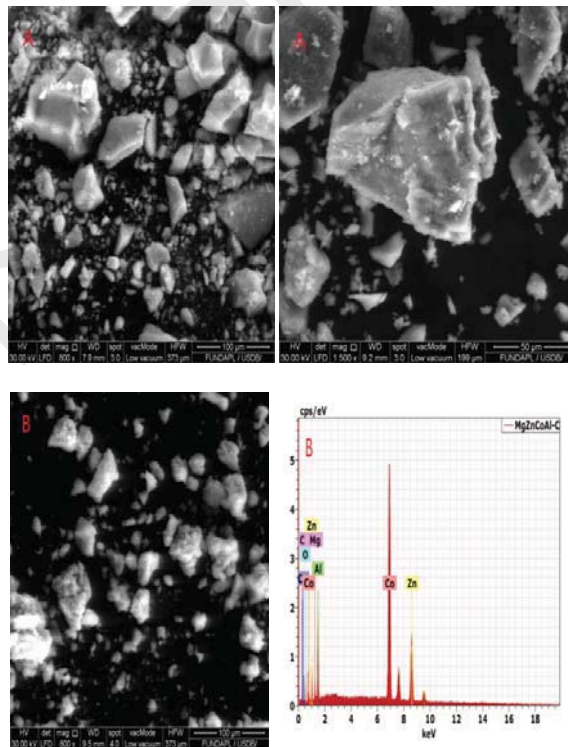


Fig . 5 .SEM micrographs of (A) MgZnCoAl-CO<sub>3</sub> (B) MgZnCoAl-C

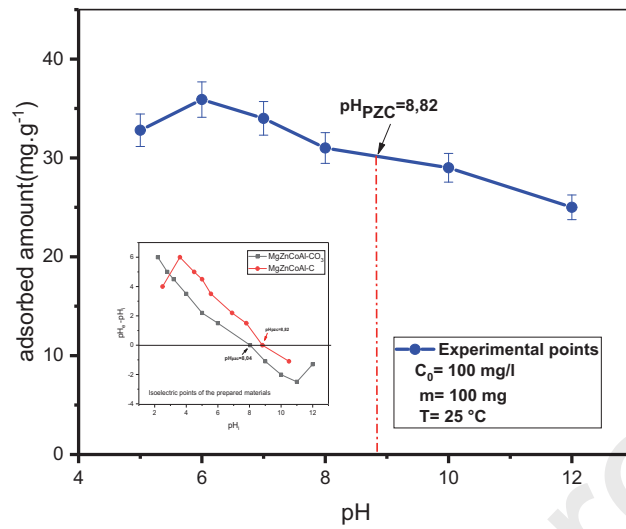


Fig 6. Effect of initial pH on adsorption of nitrate onto MgZnCoAl-C sample.

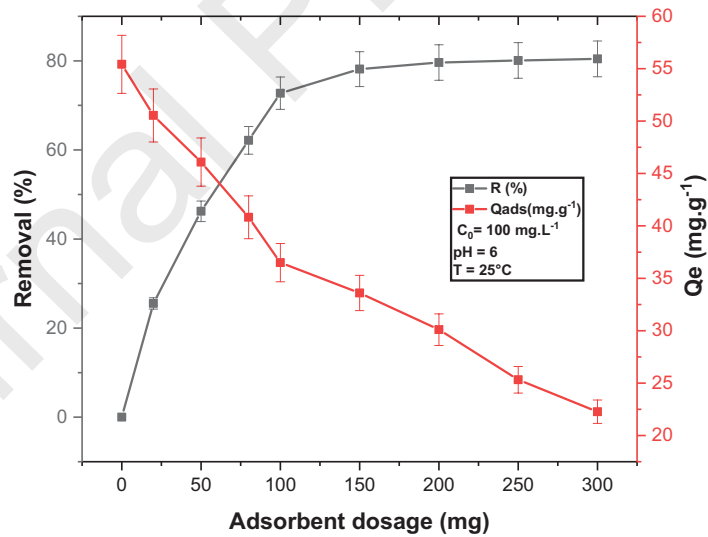
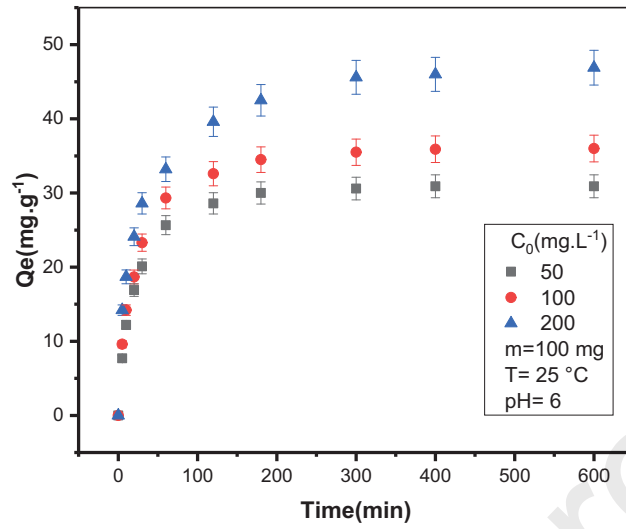
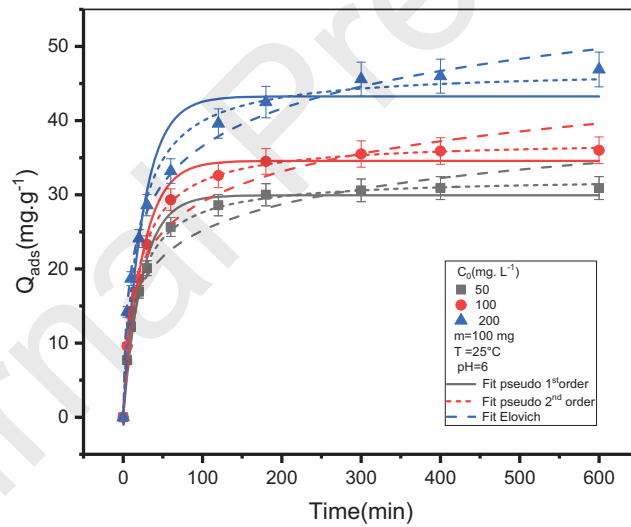


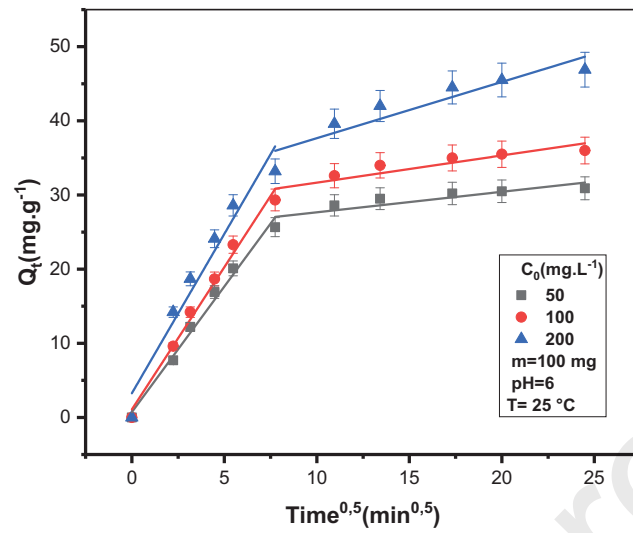
Fig.7. Effect of the adsorbent dosage on the adsorption of nitrate onto MgZnCoAl-C.



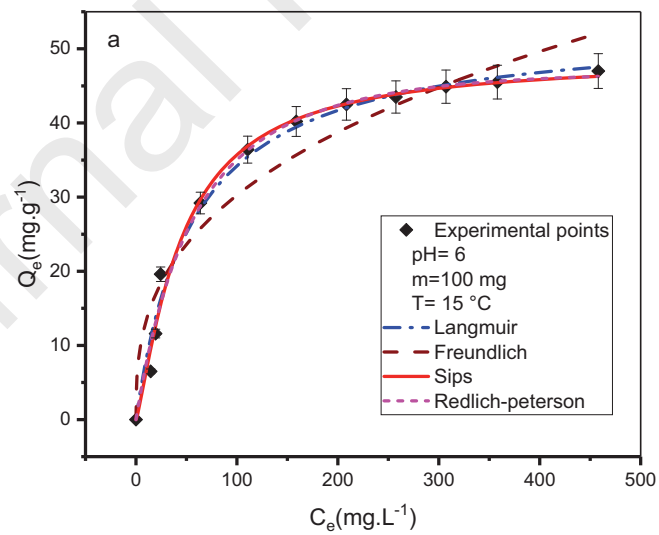
**Fig. 8.** Effect of contact time and initial nitrate concentrations onto MgZnCoAl-C



**Fig 9.** The curves representative of Nonlinear simulation of the pseudo-first-order (PFO), pseudo-second-order (PSO), and Elovich



**Fig.10.** Data fitting of the nitrate adsorption kinetics by intra-particle diffusion model onto MgZnCoAl-C at different concentrations.



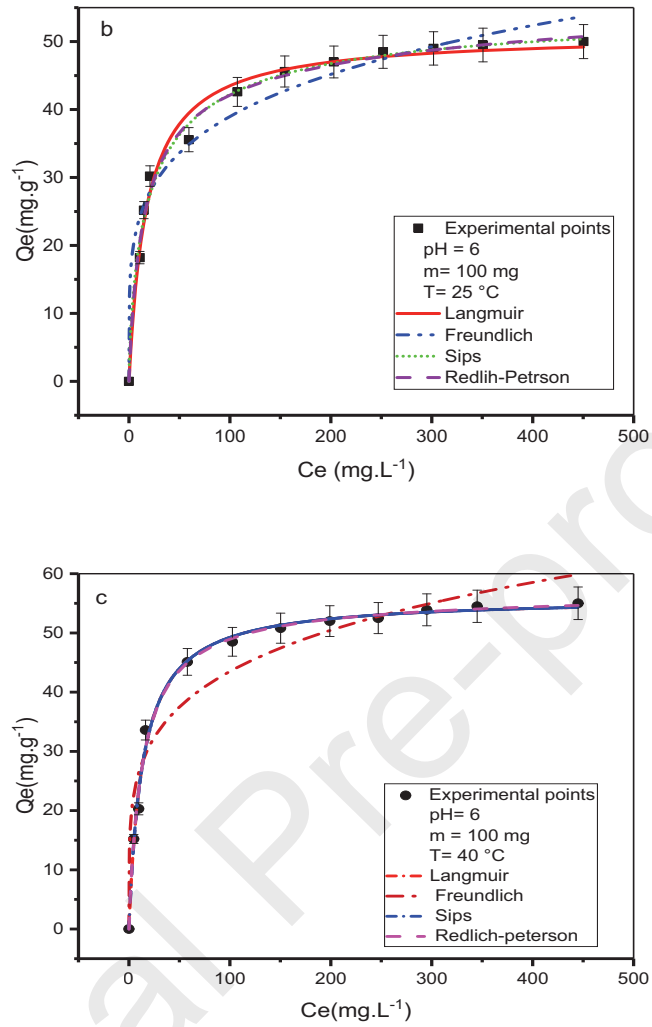
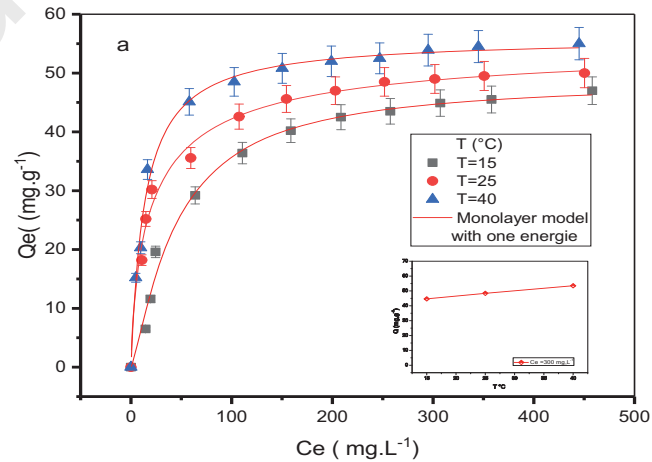
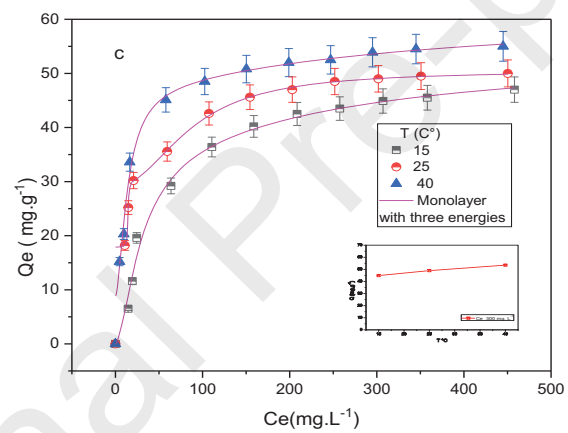
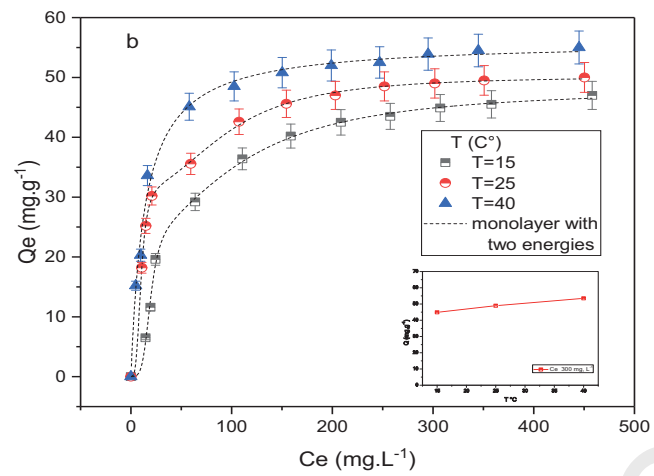
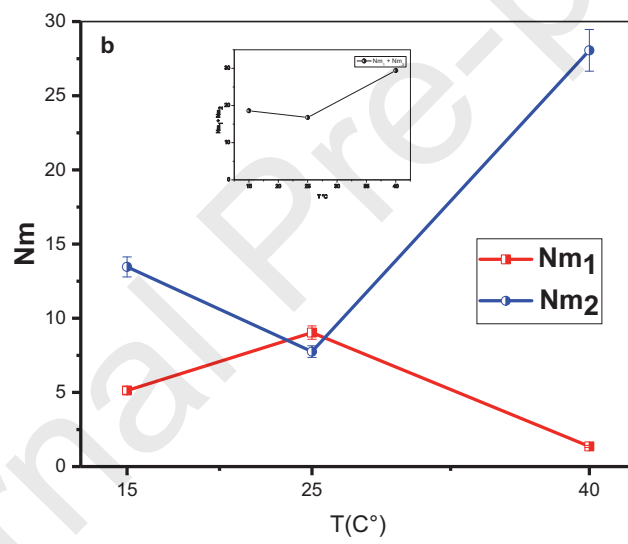
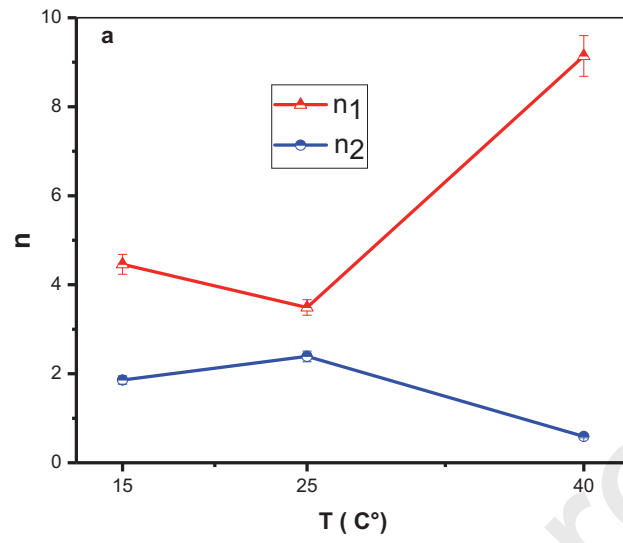


Fig.11. Adsorption isotherms, (a) 15 °C, (b) 25 °C, and (c) 40 °C





**Fig 12:** Data fitting of the nitrate adsorption isotherm by a) Monolayer with one binding site; b) Monolayer with two binding site; c) Monolayer with three binding site.



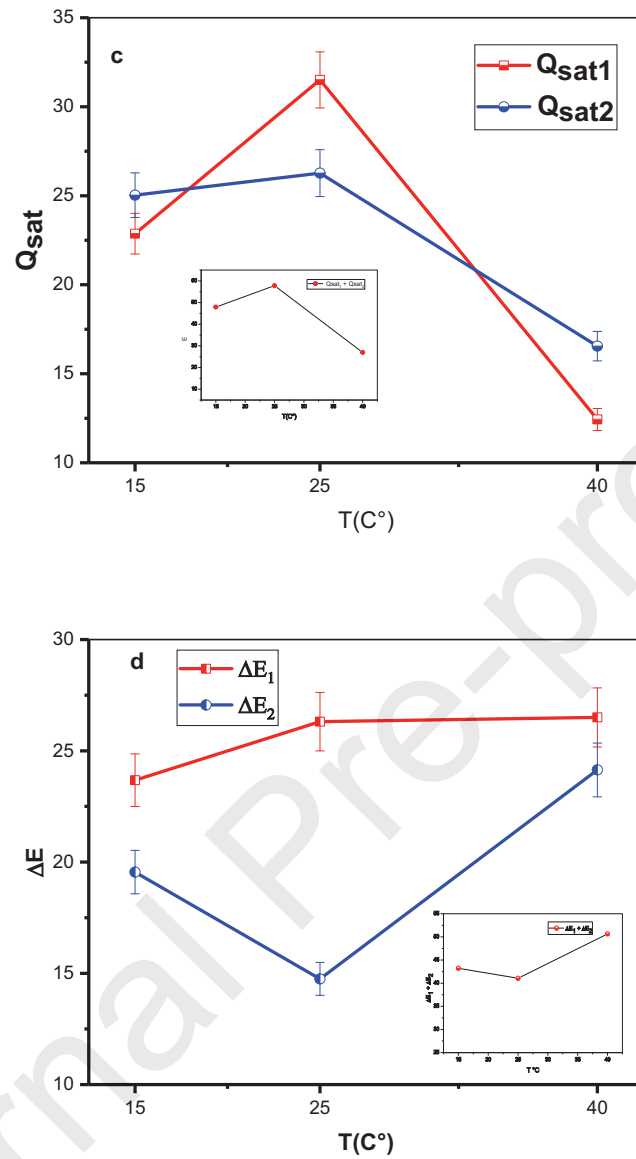


**Fig 13:** a)  $n_1$  and  $n_2$  versus temperature for the adsorption of  $\text{NO}_3$ ; b)  $N_{m1}$  and  $N_{m2}$  versus temperature for the adsorption of  $\text{NO}_3$ ; c)  $Q_{\text{sat1}}$  and  $Q_{\text{sat2}}$  versus temperature for the adsorption of  $\text{NO}_3$ ; d) Estimated adsorption energies for nitrate removal.

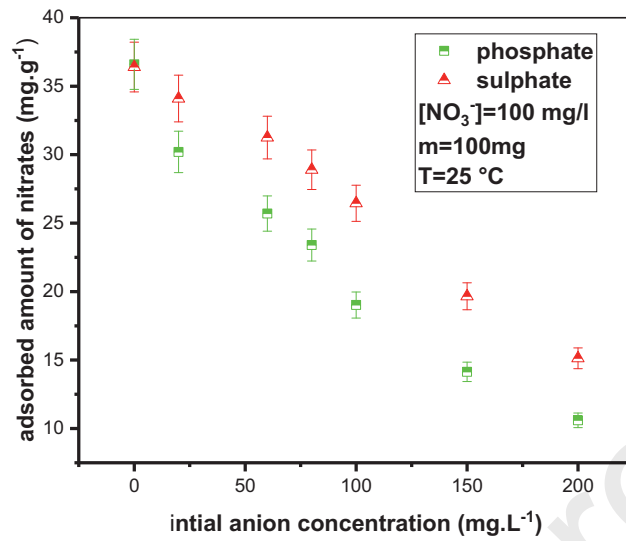


**Fig.14.** Adsorbed amount of versus initial anion concentration of solution with initial nitrate concentration of 100 mg/L.

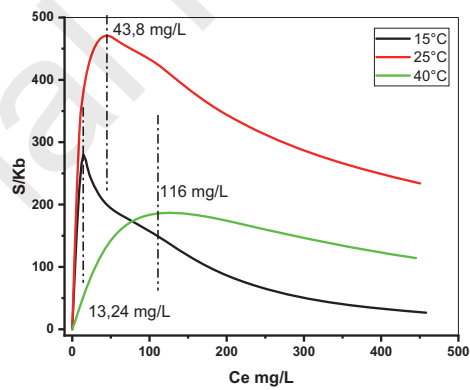


**Fig. 15.** Entropy as a feature of Ce at 15, 25, and 40 °C.

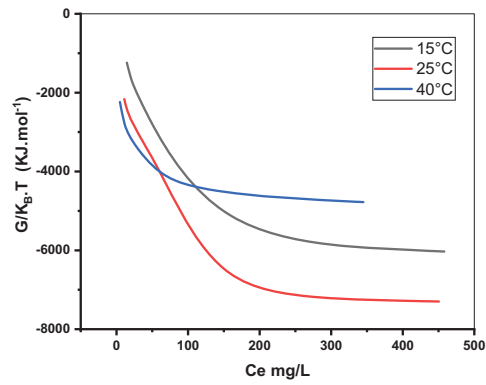


**Fig.16.** Evolution of the Gibbs Free Enthalpy at 15, 25, and 40 °C.

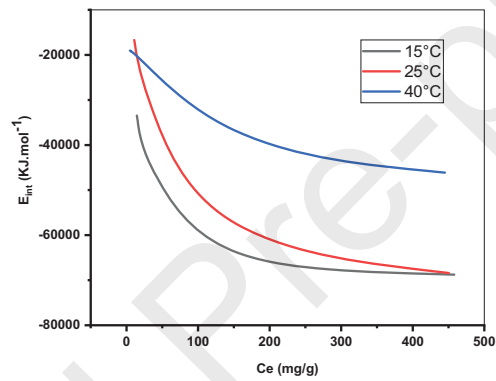


**Fig.17.** Evolution of the Internal Energy relative to the sorption system at 15 °C, 25 °C and 40°C .

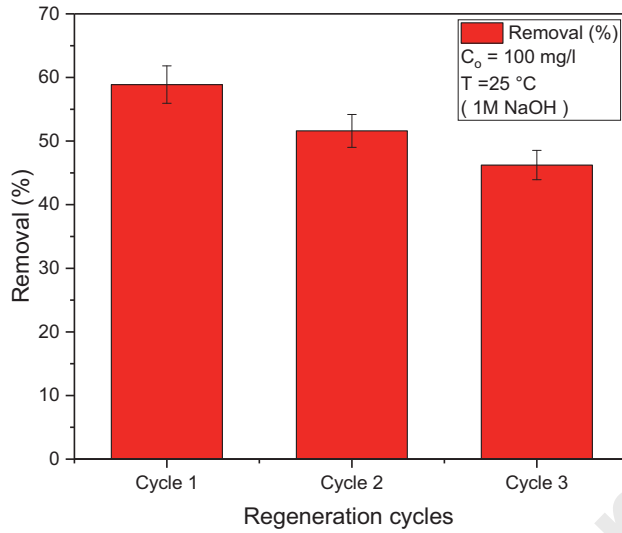


**Fig.18:** Regeneration study for MgZnCoAl-C at 1M NaOH

**Table 1:** PFO , PSO ,IPD, Elovich equations and parameters.

Kinetics model	Number	Equation	Parameters
Pseudo-first order	3	$Q_t = Q_e (1 - e^{-k_1 t})$	$Q_e$ (mg•g <sup>-1</sup> ), $k_1$ (L•min <sup>-1</sup> ),
Pseudo-second order	4	$Q_t = \frac{k_2 Q_e^2 t}{1 + k_2 Q_e t}$	$Q_e$ (mg•g <sup>-1</sup> ), $k_2$ (L•min <sup>-1</sup> )
Intraparticle diffusion	5	$Q_t = k_{id} \cdot t^{1/2} + C$	C, $k_{id}$ (mg•g <sup>-1</sup> min <sup>-0.5</sup> ),
Elovich	6	$Q_t = \frac{1}{\beta} \ln(\alpha\beta) + \frac{1}{\beta} \ln t$	$\alpha$ (mg/g min) $\beta$ (g/mg)

**Table2.** Langmuir, Freundlich, Sips and Redlich-Peterson (R-P) equations and parameters.

Isotherm model	number	Equation	Parameters
Langmuir	10	$Q_e = \frac{Q_m \cdot K_L \cdot C_e}{1 + K_L \cdot C_e}$	$Q_m, K_L$
Freundlich	11	$Q_e = K_F \cdot C_e^{\frac{1}{n}}$	$K_F, n$

Sips	12	$Q_e = \frac{Q_m \cdot K_S \cdot C_e^{m_s}}{(1 + K_S \cdot C_e^{m_s})}$	Qm, K <sub>S</sub> , m <sub>s</sub>
Redlich-Peterson	13	$Q_e = \frac{A_{RP} C_e}{1 + B_{RP} C_e^g}$	A <sub>RP</sub> , B <sub>RP</sub> , g

Table 3. The Advanced statistical physics models AM1, AM2 and AM3,

Advanced statistical physics models				
Model	Num	Equation	Parametres	Ref
Single-energy single-layer model(AM1)	17	$Q_e = \frac{n \cdot N_m}{1 + \left(\frac{C_1/2}{C_e}\right)^n}$	n, C <sub>1/2</sub> , N <sub>m</sub>	[47]
Double-energy single-layer model(AM 2)	18	$Q_e = \frac{n_1 \cdot N_{m1}}{1 + \left(\frac{C_1}{C_e}\right)^{n_1}} + \frac{n_2 \cdot N_{m2}}{1 + \left(\frac{C_2}{C_e}\right)^{n_2}}$	n <sub>1</sub> , n <sub>2</sub> C <sub>1</sub> , C <sub>2</sub> N <sub>m1</sub> , N <sub>m2</sub>	[48]
Triple-energy - single layer model (AM 3)	19	$Q_e = \frac{n_1 \cdot N_{m1}}{1 + \left(\frac{C_1}{C_e}\right)^{n_1}} + \frac{n_2 \cdot N_{m2}}{1 + \left(\frac{C_2}{C_e}\right)^{n_2}} + \frac{n_3 \cdot N_{m3}}{1 + \left(\frac{C_3}{C_e}\right)^{n_3}}$	n <sub>1</sub> , n <sub>2</sub> , n <sub>3</sub> C <sub>1</sub> , C <sub>2</sub> , C <sub>3</sub> N <sub>m1</sub> , N <sub>m2</sub> N <sub>m3</sub>	[49]

Table 4. Entropy, free enthalpy, and internal energy function according to the AM2 model.

Function	Equation	Num
Classical thermodynamics model		
	$\Delta G^\circ = -R T \cdot \ln K_D(15)$	20
	$\Delta G = DH - TDS$	21
Statistical thermodynamic model		
Entropy	$\frac{S_a}{K_B} = N_1 \left[ \ln \left( 1 + \left( \frac{C_e}{C_1} \right)^{n_{1m}} \right) + \frac{n_1 \ln \left( \frac{C_1}{C_e} \right)}{1 + \left( \frac{C_1}{C_e} \right)^{n_{1m}}} \right] + N_2 \left[ \ln \left( 1 + \left( \frac{C_e}{C_2} \right)^{n_2} \right) + \frac{n_2 \ln \left( \frac{C_2}{C_e} \right)}{1 + \left( \frac{C_2}{C_e} \right)^{n_2}} \right]$	22
Gibbs free enthalpy	$G = K_B T \ln \left( \frac{C_e}{Z_v} \right) \left[ \frac{Q_{sat1}}{1 + \left( \frac{C_1}{C_e} \right)^{n_{1m}}} + \frac{Q_{sat2}}{1 + \left( \frac{C_2}{C_e} \right)^{n_{2m}}} \right]$ $Z_v = \frac{Z_{gtr}}{V} = \left( \frac{2\pi m K_B T}{h^2} \right)^{3/2}$	23

$$E_{int} = K_B T \left[ N_{1s} \frac{\ln\left(\frac{C_e}{Z_v}\right) + n_{1m} \ln\left(\frac{C_1}{C_e}\right)}{1 + \left(\frac{C_1}{C_e}\right)^{n_{1m}}} + N_{2s} \frac{\ln\left(\frac{C_e}{Z_v}\right) + n_{2m} \ln\left(\frac{C_2}{C_e}\right)}{1 + \left(\frac{C_2}{C_e}\right)^{n_{2m}}} \right]$$

24

**Table.5.** BET parameters of prepared materials

Material	S <sub>BET</sub> (m <sup>2</sup> /g)	S <sub>ext</sub> (m <sup>2</sup> /g)	V <sub>pT</sub> (cm <sup>3</sup> /g)
MgZnCoAl-CO <sub>3</sub>		81.66	79.98
MgZnCoAl-C		102.36	89.68

**Table.6.** Kinetics model parameters for nitrate adsorption on MgZnCoAl-C and the corresponding coefficients of correlation R<sup>2</sup>

C(mg/l)	50	100	200
LDH			
<b>Experimental data</b>			
Q <sub>exp</sub> (mg.g <sup>-1</sup> )	30.9	36	46.9
<b>Pseudo-first Order model</b>			
k <sub>1</sub> (min <sup>-1</sup> )	0.0418	0.0410	0.0407
Q <sub>e</sub> (mg.g <sup>-1</sup> )	29.92	34.57	43.27
<b>R<sup>2</sup></b>	<b>0.9839</b>	<b>0.9772</b>	<b>0.9348</b>
<b>Pseudo-second Order model</b>			
k <sub>2</sub> (g mg <sup>-1</sup> min <sup>-1</sup> )	1.8110 <sup>-3</sup>	1.5410 <sup>-3</sup>	1.2210 <sup>-3</sup>
Q <sub>e</sub> (mg.g <sup>-1</sup> )	32.32	37.37	46.90

<b>R<sup>2</sup></b>	<b>0.998</b>	<b>0.996</b>	<b>0.983</b>
<b>Elovich model</b>			
$\alpha$ (g mg <sup>-1</sup> min <sup>-1</sup> )	7.101	8.210	10.820
$\beta$ (g mg <sup>-1</sup> min <sup>-1</sup> )	0.196	0.169	0.136
<b>R<sup>2</sup></b>	<b>0.961</b>	<b>0.968</b>	<b>0.991</b>
<b>Intraparticle diffusion model</b>			
$k_3$ (g mg <sup>-1</sup> min <sup>-0.5</sup> )	0.277	0.366	0.757
C	24.88	28.00	30.08
<b>R<sup>2</sup></b>	<b>0.759</b>	<b>0.807</b>	<b>0.841</b>

**Table.7.** Langmuir, Freundlich, Sips and Redlich-Peterson parameters for nitrate adsorption onto MgZnCoAl-C

T(°C)	15	25	40
LDH			
<b>Experimental data</b>			
$Q_{exp}$ (mg.g <sup>-1</sup> )	47	50	55
<b>Langmuir model</b>			
$K_L$ (L.mg <sup>-1</sup> )	0.017	0.057	0.073
$Q_e$ (mg.g <sup>-1</sup> )	53.36	51.10	55.965
$R_L$	0.37	0.15	0.12
<b>R<sup>2</sup></b>	<b>0.986</b>	<b>0.987</b>	<b>0.983</b>
<b>AIC</b>	<b>23.98</b>	<b>34.60</b>	<b>20.45</b>
<b>Ferundlich model</b>			
$K_F$ (mg g <sup>-1</sup> (L mg <sup>(1/n)</sup> ))	5.83	14.59	16.21

n	2.79	4.68	4.66
<b>R<sup>2</sup></b>	<b>0.928</b>	<b>0.967</b>	<b>0.936</b>
<b>AIC</b>	<b>43.01</b>	<b>45.50</b>	<b>43.74</b>
<b>Sips model</b>			
Q <sub>m</sub> (g mg <sup>-1</sup> )	48.80	55.54	55.97
K <sub>s</sub>	0.022	0.046	0.07
m <sub>s</sub>	1.25	0.749	0.99
<b>R<sup>2</sup></b>	<b>0.988</b>	<b>0.9907</b>	<b>0.998</b>
<b>AIC</b>	<b>23.25</b>	<b>20.54</b>	<b>17.45</b>
<b>Redlich-peterson model</b>			
A <sub>RP</sub> (L mol <sup>-1</sup> )	0.82	3.80	4.27
B <sub>RP</sub> (L mol <sup>-1</sup> )	0.008	0.10	0.08
G	1.09	0.93	0.98
<b>R<sup>2</sup></b>	<b>0.986</b>	<b>0.9901</b>	<b>0.993</b>
<b>AIC</b>	<b>26.03</b>	<b>23.54</b>	<b>20.15</b>

**Table. 8 .** Comparison of adsorption capacities of layered double hydroxide for nitrate removal.

Sample LDH	Nitrate removal (%)	Reference
Uncalcined Mg/Fe/Cl	69.95	[75]
Mg/Al/CO <sub>3</sub> (500 °C)	74	[79]
Mg/Al/CO <sub>3</sub> (550 °C)	70.4	[12]
Zn/Al/CO <sub>3</sub> (550 °C)	25	[80]
Uncalcined Mg/Al/Cl	89	[7]
Uncalcined Mg/Fe/Cl	72.6	
Uncalcined Zn/Al/Cl	89.9	[71]
Ca/Al/Cl(400 °C)	84.6	[38]
Mg/Al/CO <sub>3</sub> (500 °C)	66.4	[55]
MgZnCoAl-C (500°C)	72.73	This study

Table .9. Calculated parameters of the monolayer adsorption model with one binding sites for nitrate adsorption onto MgZnCoAl-C.

Parameters	T=15 (°C)	T=25 (°C)	T=40 (°C)
n	1.25	0.749	0.999
$N_m$	38.00	72.00	56.00
$Q_{sat}$	47.5	53.28	55.94
$C_{1/2}$ (mg L <sup>-1</sup> )	44.9	21.47	13.63
$\Delta E$ (kJ mol <sup>-1</sup> )	21.46	22.21	23.32
$R^2$	0.988	0.990	0.993

Table .10. Calculated parameters of the monolayer adsorption model with two binding sites for nitrate adsorption onto MgZnCoAl-C.

Parameters	T=15 (°C)	T=25 (°C)	T=40 (°C)
$n_1$	4.46	3.49	9.14
$n_2$	1.86	2.39	0.59
$N_{m1}$	5.13	9.03	1.36
$N_{m2}$	13.46	7.75	28.06
$Q_{sat1}$	22.87	31.51	12.43
$Q_{sat2}$	25.03	26.27	16.55
$C_1$ (mg L <sup>-1</sup> )	19.13	9.97	14.14
$C_2$ (mg L <sup>-1</sup> )	106.56	96.86	18.32

$\Delta E_1(\text{kJ mol}^{-1})$	23.68	26.31	26.05
$\Delta E_2(\text{kJ mol}^{-1})$	19.55	14.75	24.14
$R^2$	0.997	0.9993	0.9998

Table .11. Calculated parameters of the monolayer adsorption model with three binding sites for nitrate adsorption onto MgZnCoAl-C.

Parameters	T=15 (°C)	T=25 (°C)	T=40 (°C)
$n_1$	10.070	4.122	1.957
$n_2$	2.464	2.813	0.708
$n_3$	3.852	5.087	0.977
$N_{m1}$	0.814	1.209	18.038
$N_{m2}$	4.606	12.253	14.570
$N_{m3}$	7.576	2.113	20.322
$Q_{sat1}$	8.196	4.204	35.15
$Q_{sat2}$	9.987	34.45	10.31
$Q_{sat3}$	29.14	10.71	19.85
$C_1 (\text{mg L}^{-1})$	101.68	221.23	13.841
$C_2 (\text{mg L}^{-1})$	237.10	10.376	4.640

$C_3$	20.824	87.535	444.89
$\Delta E_1$	19.57	17.66	24.45
$\Delta E_2$	17.61	25.08	27.25
$\Delta E_3$	23.40	19.88	15.98
$R^2$	0.997	0.980	0.989

Table.12. Thermodynamic parameters

	$\Delta G^\circ$ (KJ/mol)			$\Delta H^\circ$ (KJ/mol)	$\Delta S^\circ$ (J/mol K)
	15 °C	25 °C	40 °C	50 °C	
				14.81	59.04
	-2.18	-2.77	-3.65	-4.24	

Table 13. Maximum adsorption capacity of some adsorbents for nitrate removal from aqueous solution.

Adsorbent	pH	Isotherm	Kinetic	$Q_m$ (mg/g)	ref
Nano-alumina	4.4	Langmuir	Pseudo-second-order	4.0	[26]
Activated carbon	3.0	Langmuir	Pseudo-second-order	27.55	[81]
Raw wheat residue	6.8	Freundlich	Pseudo-second-order	1.24	[28]
Chitosan hydrogel beads	3.0	Freundlich	Pseudo-second-order	89.3	[82]
Powdered activated carbon	5.0	Freundlich	Pseudo-second-order	620	[83]
Granular chitosan –Fe <sup>3+</sup> complex	3.0-10	Langmuir	Pseudo-second-order	5.0	[84]
ZnCl <sub>2</sub> treated coconut granular activated carbon	5.5	Langmuir	Pseudo-second-order	0.2	[85]

Modified wheat residue	6.8	Freundlich	Pseudo-second-order	128.9	[28]
Granular activated carbon modified with fenton reagents	4	Freundlich		620	[86]
MgZnCoAl-LDH	6	Langmuir	Pseudo-second-order	55.97	This study

---

### Authors Contributions:

All authors contributed to the study conception and design. Material preparation, data collection and analysis were performed by Mounira Elhachmi<sup>1</sup>, Zoubida Chemat and CHEBLI Derradji. The first draft of the manuscript was written by CHEBLI Derradji, BOUGUETTOUCHA Abdallah and AMRANE Abdeltif and all authors commented on previous versions of the manuscript. All authors read and approved the final manuscript.

### Declaration of interests

The authors declare that they have no known competing financial interests or personal relationships that could have appeared to influence the work reported in this paper.

The authors declare the following financial interests/personal relationships which may be considered as potential competing interests: